JAERI-M
9834

HEAT LOSS AND FLUID LEAKAGE TESTS OF THE ROSA-III FACILITY

December 1981

Mitsuhiro SUZUKI, Kanji TASAKA
and Masayoshi SHIBA

日本原子力研究所
Japan Atomic Energy Research Institute

JAERI-Mレポートは，日本原子力研究所が不定期に公刊している研究報告書です。
入手の問合わせは，日本原子力研究所技術情報部情報資料課（〒319-11茨城県那珂郡東海村）あて，お申しこしください。なお，このほかに財団法人原子力弘済会資料センター（〒319-11 茨城県那珂郡東海村日本原子力研究所内）で複写による実費頒布をおこなっております。

JAERI-M reports are issued irregularly.
Inquiries about availability of the reports should be addressed to Information Section, Division of Technical Information, Japan Atomic Energy Research Institute, Tokai-mura, Naka-gun, Ibaraki-ken 319-11, Japan.

編集兼発行　日本原子力研究所
印　　刷　いばらき印刷㈱

JAERI-M 9834

Heat Loss and Fluid Leakage Tests of the ROSA-III Facility

Mitsuhiro SUZUKI, Kanji TASAKA
and Masayoshi SHIBA

Division of Reactor Safety,
Tokai Research Establishment, JAERI

(Received November 16, 1981)

The report presents characteristic test results about the steady state heat loss, one of the inherent characteristics of the ROSA-III test facility. The steady state heat loss tests were conducted at five different temperature conditions between 111°C and 290°C. Net heat loss rates were obtained by estimating the electric power supplied to the core, heat input from the recirculation pumps and steam leakage rate. The heat loss characteristics have important contribution to analyses of the ROSA-III small break tests.

A following simple relation was obtained between the net heat loss rate $\dot{Q}_{HL}$ (kJ/s) of the ROSA-III facility and the temperature difference ΔT (°C) between the fluid temperature of the system and the room temperature,

$$\dot{Q}_{HL} = 0.56 \times \Delta T.$$

And the steam leak flow at normal operating condition of the ROSA-III test, (P = 7.2 MPa) was obtained as 8.9×10^{-3} kg/s and corresponding steam leakage energy as 10.5 kJ/s. The heat input from the recirculation pumps was indirectly estimated under a constant speed by assuming the heat input was equal to the brake horce power of the pumps.

Keywords; BWR, LOCA, ROSA-III Program, Integral Test Facility, Characteristics Test, Heat Loss, Steam Leakage, Recirculation Pumps

ROSA－Ⅲ装置の熱損失及び蒸気漏洩試験

日本原子力研究所東海研究所安全工学部
鈴木光弘・田坂完二・斯波正誼

（1981年11月16日受理）

本報告書は，ROSA－Ⅲ試験装置固有の特性の一つである，定常状態における熱損失に関する特性試験の結果をまとめたものである。定常熱損失試験は，111℃から290℃までの5つの異なる温度条件で行なわれた。正味の熱損失速度は，炉心での電気的熱出力と再循環ポンプからの熱入力，および蒸気漏洩量を評価することによって得た。この熱損失特性は，ROSA－Ⅲの小破断実験の解析の際に重要な役割を果すものである。

ROSA－Ⅲ装置の正味熱損失量$\dot{Q}_{HL}$（kJ／s）と，流体温度と室温の温度差ΔT（℃）との間に，次の簡単な関係式が得られた。

$$\dot{Q}_{HL} = 0.56 \times \Delta T$$

また，ROSA－Ⅲ試験の通常運転条件（P＝7.2 MPa）における蒸気漏洩速度は，8.9×10^{-3} kg/sおよびこれに対応する蒸気漏洩エネルギー速度は10.5 kJ／s であった。再循環ポンプからの熱入力は，一定回転速度条件下において，ポンプ軸動力に等しいと仮定することによって間接的に求めた。

Contents

目　　次

Tables and Figures

1. Introduction

The ROSA-Ⅲ program is one of several water reactor research test programs conducted by JAERI (Japan Atomic Energy Research Institute). The ROSA-Ⅲ facility[1] is an integral test facility designed to simulate a loss-of-coolant accident (LOCA) of a BWR/6 and to evaluate the effectiveness of engineered safety features during a LOCA. The objectives of the ROSA-Ⅲ program are:

(1) To provide LOCA experiment data required to assess and improve the analytical codes,

(2) To identify and investigate any unexpected events or threshholds in the response of the plant and/or the engineered safety features and to develop the analytical models for them.

In order to meet these objectives, several characteristic tests or performance tests have been performed for the ROSA-Ⅲ test facility and its components in addition to the integral tests. The characteristic tests results are reported for the jet pump performance in normal and reverse flow[2], the correlation between conduction probe signals and liquid level or void fraction[3], and the single phase pump head characteristics of the recirculation pumps[4].

Heat loss at the steady state of the ROSA-Ⅲ facility is one of the important characteristics of the system, especially in the case of small break LOCA tests and their analyses, because the heat loss rate becomes comparable with heat generation rate in the core at long time after break. The heat loss tests are conducted at constant fluid temperature by controlling the electric power supplied to the core. In order to estimate the net heat loss rate through the pressure boundary of the system, heat input from the operating recirculation pumps (MRP-1 and 2) and energy leakage rate due to steam leak flow must be estimated in addition to the thermal output in the core. As the recirculation pumps MRP-1 and MRP-2 of the ROSA-Ⅲ facility are centrifugal non-seal type pumps (canned type), the brake horse powers of the pumps can be given by subtracting the heat removal rate at the motor part from the electric power supplied to the motor. And the brake horse power is transformed into three components, namely the hydraulic power, frictional power between the fluid and the pump rotating parts and the heat loss through the pump casings to atmosphere. The heat loss at the pump is a part of total heat loss in the

system. Then the heat input from two recirculation pumps can be given as two times of the brake horse power per one pump. To know accurately the brake horse power, however, is not so easy because of rough measurements of the cooling water flow rate and of very small temperature difference across the pump motor part. Therefore, the brake horse power of the pump is estimated indirectly in the heat loss test by using the data of the report of inspection test results on the ROSA-III facility[5], where the brake horse power of the pump was estimated by using theoretical pump efficiency as shown in chapter 4.

The steam leakage flow rate is observed by the water level change in the pressure vessel. As the water level change in each heat loss test was very small, a steam leakage test with long test periods was planned at the last phase of heat loss tests as shown in the section 3.2. The heat loss tests and the leakage test were performed on September 9 and October 3, 1980.

In these calorimetric tests, achievement of thermal steady condition in the system has important effects on the accuracy of the steady heat loss rate. This effect is discussed in chapter 5 using a theoretical solution of one-dimensional heat conduction in the case of sudden temperature rise at one side of a thick flat plate with insulation condition at the other side as shown in the appendix.

2. Test Facility and Test Procedures

2.1 The ROSA-III Test Facility and Measurements

The ROSA-III facility is composed of the pressure vessel with internals, two recirculation loops with two recirculation pumps (MRP-1 and MRP-2) and other pipings for steam discharge lines, ECCS and feed water systems, as shown in Fig. 2.1. Major design characteristics of the pressure vessel, pipings and recirculation pumps are listed in Table 2.1.

The pressure vessel shown in Fig. 2.2 is devided into three parts, the upper part above the elevation 4.412 m from the bottom of the vessel, the main lower part and the bottom flange attached with leading rods for the electric heater rods in the core. Each part is tightly attached each other by bolts and nuts. Total weight of the pressure vessel with nozzles but without internals is 1.26×10^4 kg. Inner surface area of the vessel

system. Then the heat input from two recirculation pumps can be given as two times of the brake horse power per one pump. To know accurately the brake horse power, however, is not so easy because of rough measurements of the cooling water flow rate and of very small temperature difference across the pump motor part. Therefore, the brake horse power of the pump is estimated indirectly in the heat loss test by using the data of the report of inspection test results on the ROSA-III facility[5], where the brake horse power of the pump was estimated by using theoretical pump efficiency as shown in chapter 4.

The steam leakage flow rate is observed by the water level change in the pressure vessel. As the water level change in each heat loss test was very small, a steam leakage test with long test periods was planned at the last phase of heat loss tests as shown in the section 3.2. The heat loss tests and the leakage test were performed on September 9 and October 3, 1980.

In these calorimetric tests, achievement of thermal steady condition in the system has important effects on the accuracy of the steady heat loss rate. This effect is discussed in chapter 5 using a theoretical solution of one-dimensional heat conduction in the case of sudden temperature rise at one side of a thick flat plate with insulation condition at the other side as shown in the appendix.

2. Test Facility and Test Procedures

2.1 The ROSA-III Test Facility and Measurements

The ROSA-III facility is composed of the pressure vessel with internals, two recirculation loops with two recirculation pumps (MRP-1 and MRP-2) and other pipings for steam discharge lines, ECCS and feed water systems, as shown in Fig. 2.1. Major design characteristics of the pressure vessel, pipings and recirculation pumps are listed in Table 2.1.

The pressure vessel shown in Fig. 2.2 is devided into three parts, the upper part above the elevation 4.412 m from the bottom of the vessel, the main lower part and the bottom flange attached with leading rods for the electric heater rods in the core. Each part is tightly attached each other by bolts and nuts. Total weight of the pressure vessel with nozzles but without internals is 1.26×10^4 kg. Inner surface area of the vessel

is 12.4 m^2 assuming no nozzles on the vessel. Metal volume of the pressure vessel with nozzles can be determined as 1.61 m^3, by using the specific weight 7.82×10^3 kg/m^3 of the vessel made of stainless steel (SUS 304). Average wall thickness of the vessel can be estimated as 0.13×10^{-1} m by dividing the metal volume by the inner surface area. The outer surface of the vessel is covered with thermal insulator made of glass wool except for the nozzles, flanges and the attachments for supporting. The heat leaks primarily from the pressure vessel through the un-insulated flanges, nozzles and attachments. Especially, the bottom flange with many leading rods of electrical heaters, the upper two flanges connecting the upper part and the main part of the vessel may have a large contribution to the heat loss. The thermal insulator around the pressure vessel has 0.1 m thickness and it is covered with thin metal plate.

The pressure vessel contains the following internals which do not contribute to the heat loss when the system is in the thermal steady state. Major internals are steam separator, core shroud, filler blocks, four simulated fuel assemblies in the core, guide tube and the internal pipings for ECCS and feed water. Most of these internals are made of stainless steel (SUS 304) and have thickness (or diameter) less than 12.5 mm.

There are two recirculation loops in the ROSA-III facility. The intact loop has two jet pumps JP-1 and 2 as shown in Fig. 2.3 installed outside the pressure vessel and a recirculation pump MRP-1. Similarly, the broken loop has two jet pumps JP-3 and 4, a recirculation pump MRP-2 and two break units. Main structural design values of the two loops are shown in Table 2.2. Total lengths of the intact and broken loops are 31.5 m and 38.0 m, respectively. Total inner surface area of the two recirculation loops was estimated as 11.3 m^2 assuming the jet pumps, recirculation pumps and the Venturi flow meters as 2B pipings (Sch. 80), jet pump discharge lines as 3B pipings (Sch. 80) and jet pump suction lines as $1\frac{1}{2}$B pipings as shown in Table 2.2 for the sake of simplification. Total weight of the two loops was estimated 6180 kg as the sum of the weights of four jet pumps (SUS 304, 60 kg per one pump), two recirculation pumps (SUS 304, 1600 kg per one pump) and all the pipings assuming as 2B piping without flanges and nozzles. Most part of the two loops are covered with glass wool thermal insulator of 50 mm thickness except for nozzles, flanges, recirculation pumps and break units. The thermal

insulator is surrounded by thin metal covers.

In the heat loss tests and leakage test, two types of measurements are used. One is the short time measurements (See Table 3.1) at each steady test condition recorded by digital DATAC 2000B system and the other one is the long time measurements of controlling system recorded by pen-recorders including the heating-up process. Achievement of each thermal steady condition is judged in the tests by the latter measuring system.

Table 2.1 Primary Characteristics of the ROSA-III Facility

a) Comparison of Major Design Parameters

	BWR6(251/848)	ROSA-III	Ratio($\frac{BWR6}{ROSA-III}$)
Reactor Type	BWR	Simulated BWR	
Number of			
Recirc. Loops	2	2	1
Steam Lines	4	1	4
Jet Pumps	24	4	6
Separators	212	1	212
Core Heat Generation	Nuclear Fission	Electric Heater	
Total Power(kW)	3.80×10^5	< 4450	> 854
Active Fuel Length(m)	3.759	1.880	2
Number of Fuel Assemblies	848	4	212
Total Volume(m^3)	621	1.42	437
Operating Conditions			
Pressure(MPa)	7.27	7.27	
Core Flow(kg/s)	1.54×10^4	< 3.64	> 424
Steam Flow(kg/s)	2.06×10^3	< 4.86	> 424
Recirc. Pump Flow Rate per 1 Pump (kg/s)	2.24×10^3	< 5.26	> 424
Feed Water Temp.(K)	489	489	1

Table 2.1 (continued)

b) Volume Distribution and Main Component Dimension

Item		BWR6(251/848)	ROSA-III	Ratio($\frac{BWR6}{ROSA-III}$)
Lower Plenum & Guide Tubes	m^3	123	0.177	695
Lower Plenum	m^3	79.0	0.112	705
Guide Tubes	m^3	43.8	0.0651	673
Core	m^3	59.8	0.134	446
Core in Channels	m^3	35.4	0.0814	435
Core Bypass	m^3	24.4	0.0524	465
Upper Plenum & Steam Separators	m^3	80.5	0.185	435
Upper Plenum	m^3	52.5	0.124	423
Steam Separators	m^3	28.0	0.0610	459
Steam Dome *1)	m^3	206	0.439	468
Downcomer *2)	m^3	123	0.233*3)	528
Above Jet Pump Suction	m^3	74.2*	0.164*4)	452
Between Jet Pump Suction and Recirculation Outlet	m^3	36.8*	0.0600*3)	613
Below Recirculation Outlet	m^3	12.2	0.00900	1360
Recirculation Loops & Jet Pumps	m^3	29.6	0.171*4)	173
Total Volume	m^3	621	1.421	437
Pressure Vessel Dimension				
Inner Height	m	22.3*	6.01	3.71
Inner Diameter	m	6.38*	0.492*5)	13.0
Water Level	m	14.1*	4.62	3.04
Jet Pump Suction Level	m	8.28*	2.82	2.93
Lower Core End Level	m	5.49*	1.60*6)	3.43
Recirculation Line Level	m	3.88*	0.938	4.13
Recirculation Loop Pipe Inner Diameter	m	0.54	$\leq$0.0495	

Note : * BWR 5
*1)above normal water level
*2)below normal water level
*3)include jet pump suction lines
*4)not include jet pump suction lines
*5)out diameter of lower downcomer
*6)bottom of active fuel

Table 2.2 Piping design parameters of two recirculation loops of the ROSA-Ⅲ facility

Components	Pipe Type / Wall Thickness (mm)	Length (m)	Inner Surface Area (m^2)	Included Components
Ⅰ. Intact Loop				
・Downcomer Bottom to MRP-1 Suction	2B / 5.5	5.83	0.907	
・Pump MRP-1	2B*	(0.5)	(0.078)	
・MRP-1 Discharge to Top of JP-1 and 2	2B / 5.5	11.93	1.855	Venturi Flow Meter (ℓ=0.47 m)
・Top of JP-1 and 2 to Drive Nozzles	$1\frac{1}{2}$B / 5.1	1.64	0.198	
・JP-1 and JP-2	2B*	2.86	(0.445)	
・JP-1 and 2 Discharge to L.Plenum Inlet	3B* / 7.6	5.68	(1.319)	2B pipe (ℓ=1.14 m)
・Middle Downcomer to JP-1 and 2 Suction	$1\frac{1}{2}$B* / 5.1	3.10	(0.374)	$2\frac{1}{2}$B pipe (ℓ=1.30 m)
Total		(31.54)	(5.176)	
Ⅱ. Broken Loop				
・Downcomer Bottom to MRP-2 Suction	2B / 5.5	14.19	2.207	Break Units, Quick Shut Valve
・Pump MRP-2	2B*	(0.5)	(0.078)	
・MRP-2 Discharge to Top of JP-3 and 4	2B / 5.5	9.98	1.552	Venturi Flow Meter (ℓ=0.47 m)
・Top of JP-3 and 4 to Drive Nozzles	$1\frac{1}{2}$B / 5.1	1.64	0.198	
・JP-3 and JP-4	2B*	3.30	(0.513)	
・JP-3 and 4 Discharge to L.Plenum Inlet	3B* / 7.6	5.24	(1.217)	2B pipe (ℓ=0.70 m), Valve
・Middle Downcomer to JP-3 and 4 Suction	$1\frac{1}{2}$B* / 5.1	3.10	(0.374)	$2\frac{1}{2}$B pipe (ℓ=1.30 m)
Total		(37.95)	(6.139)	
Ⅲ. Sum of Two Loops		(69.49)	(11.315)	

* Complicated configurations of the components and the pipings are assumed to be pipings shown in the Table.

( ) Shows estimated values of the length or the inner surface area.

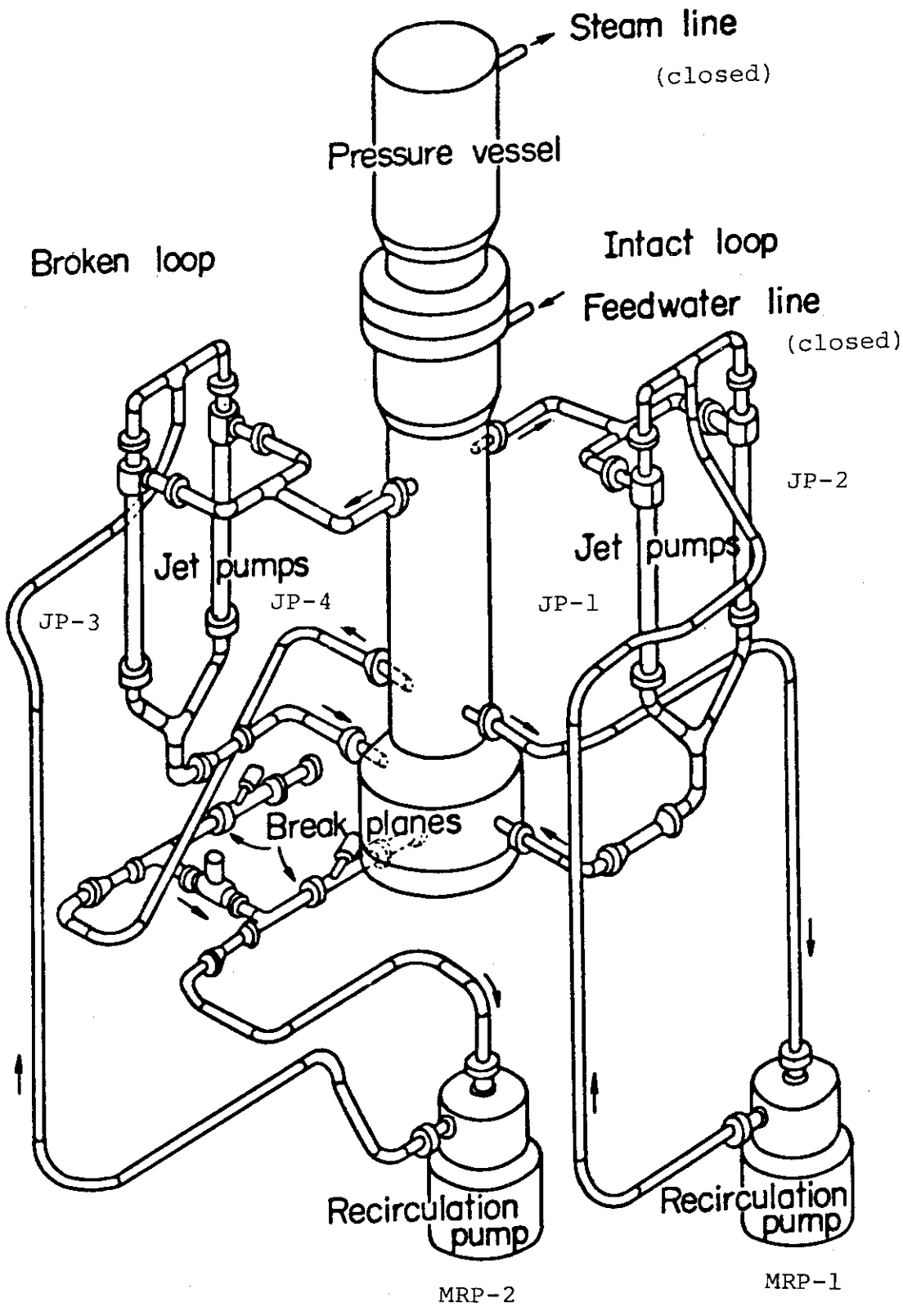

Fig. 2.1 Schematic diagram of the ROSA-III test facility

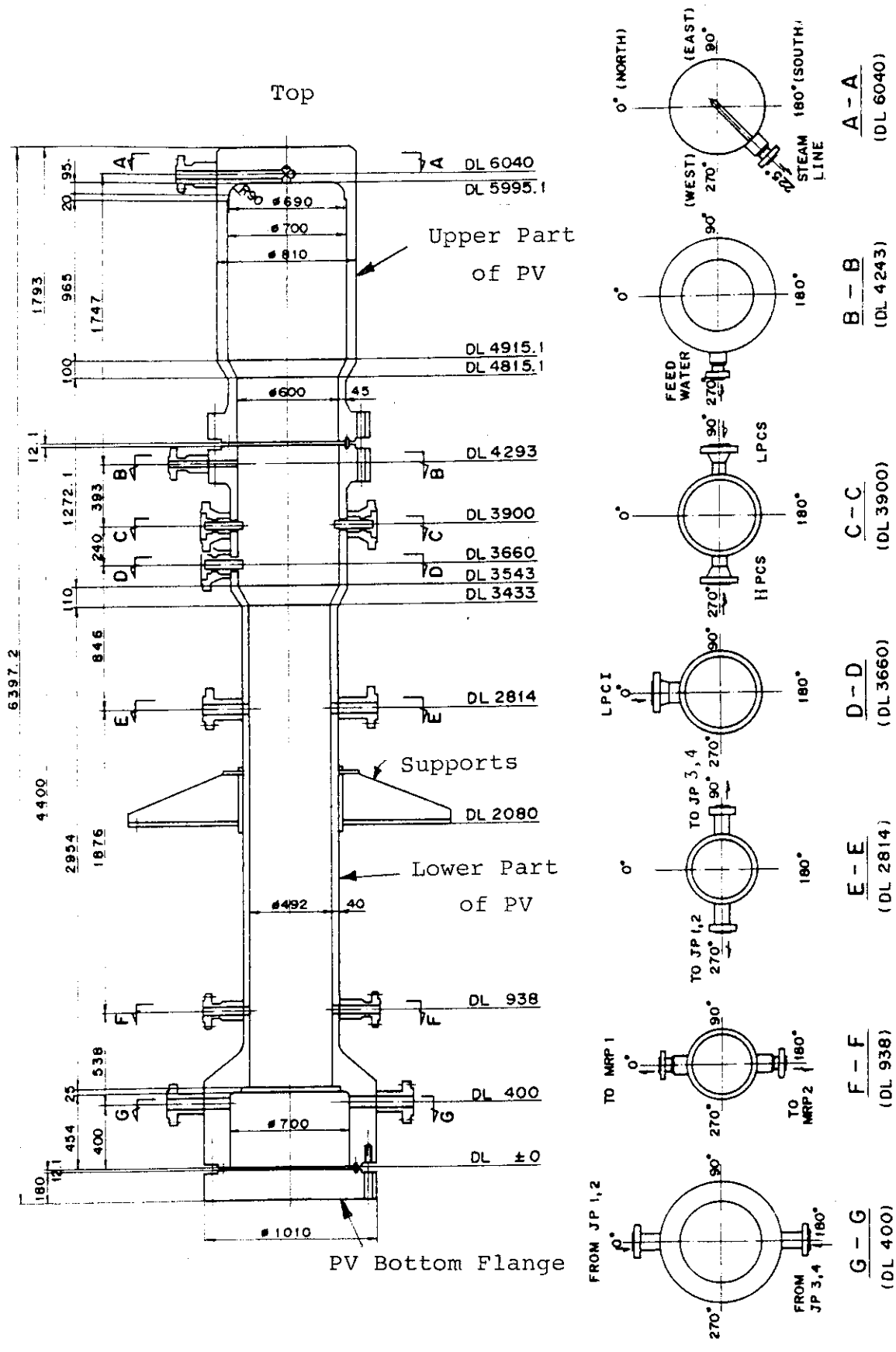

Fig. 2.2 Pressure vessel with nozzles

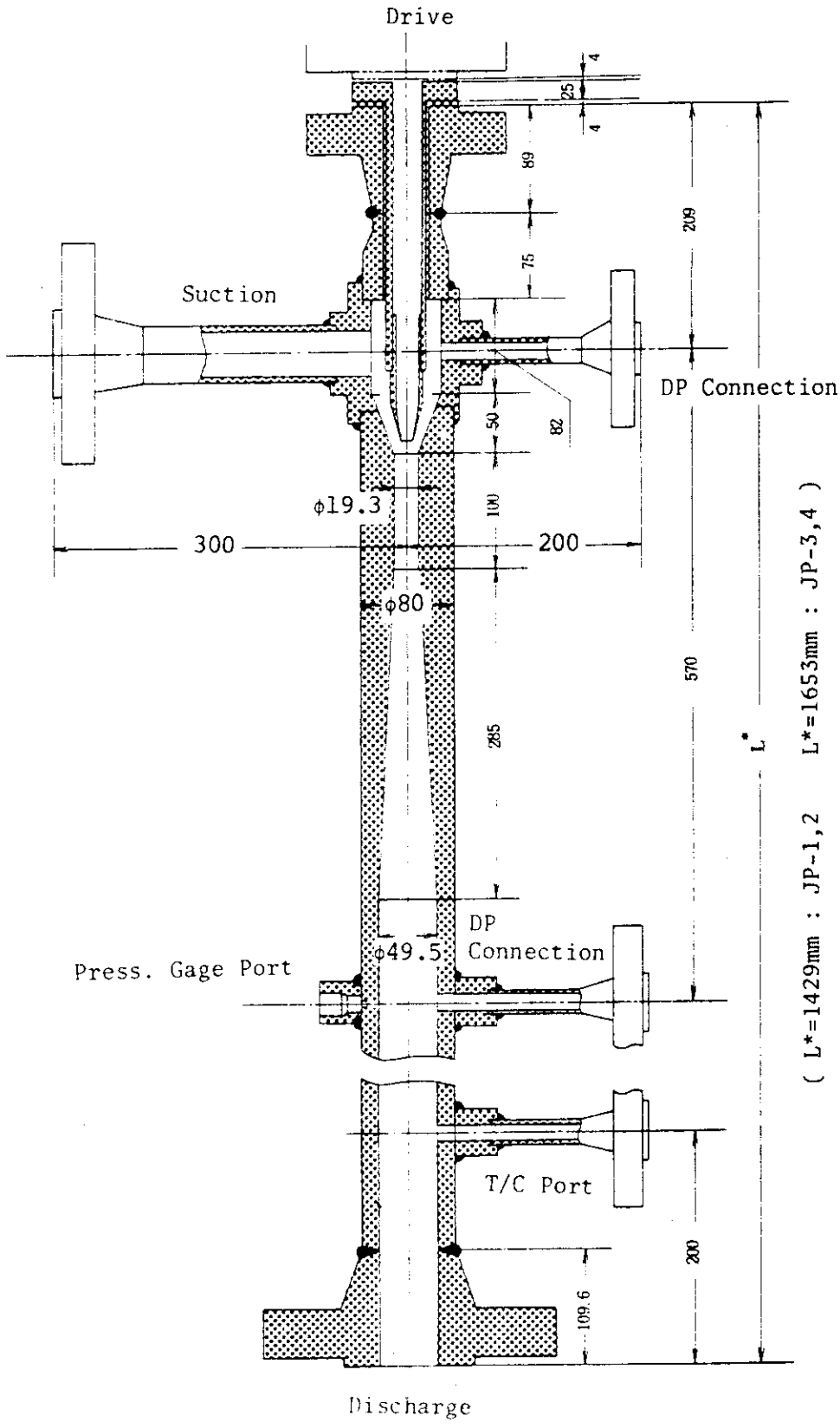

Fig. 2.3 Jet pump structure

2.2 Test Procedures

The heat loss tests and leakage test are performed in the following way. The heat loss tests are performed at five different saturated conditions of fluid temperature 111°C through 290°C. A leakage test with long test periods is performed at the highest temperature condition (290°C).

All the pipings connected to the ROSA-III pressure vessel are closed except the recirculation loops and those for measurements. Namely, the included pure water in the pressure vessel and recirculation loops makes a closed fluid system. The fluid in the system is heated up to the desired temperature condition by supplying electric power to the simulated fuel assembly in the core and by working recirculation pumps MRP-1 and MRP-2 at constant speed 209 rad/s (2000 rpm). The recirculation pumps contribute to the tests not only by establishing the homogeneous fluid conditions in the system but also by supplying heat input to the fluid. After arriving at the desived saturated temperature condition, the fluid system is maintained at the same temperature for about 30 minutes in order to make thermal steady state. As the pressure measurement in the steam dome is more accurate than the fluid temperature measurements, the pressure is kept constant at each test condition. The electric power in the core decreases to a certain value as the structural metals of the system approach the thermal steady conditions. Each heat loss test is performed after detecting the stable core electric power and the test conditions are recorded for 10 seconds in a magnetic tape by the DATAC 2000B system, such as fluid temperature, pressure, core electric power, water level in the pressure vessel, pump speed and fluid flow rate.

One leakage test is conducted for an hour in the same way as the heat loss tests. At the last phase of heat loss tests, the fluid system is maintained for an hour at the constant pressure by controlling the electric power in the core and the water level change is detected by the differential pressure transducer. The steam discharge lines and other pressure boundaries are watched whether fluid leaks or not. Test conditions in the leakage test are recorded by the same DATAC 2000B system as the heat loss tests.

3. Test Results

3.1 Net Heat Loss Rate of the ROSA-III Facility

The heat loss tests were conducted at five different fluid temperatures 111°C, 152°C, 197°C, 249°C, 288°C (290°C). The system pressure range in the heat loss tests covers from 0.14 MPa to 7.24 MPa. The heating-up process and each heat loss test time are shown in Fig. 3.1 and 3.2. These figures show steam dome temperature histories rocorded by pen-recorder through the heat loss tests. It took more than 4 hours for heating the fluid system from 100°C to 288°C (290°C). The heat loss tests were conducted after holding periods at the constant fluid temperatures. The holding periods were longer than 27 minutes. Major test conditions of each heat loss test were recorded by DATAC 2000B system as shown in Table 3.1.

There are four terms expressing the energy balance of the ROSA-III facility in a thermal steady state, namely the heat generation rate in the core ($\dot{Q}_C$), the heat input rate from the operating recirculation pumps ($\dot{Q}_B$), the energy leakage rate due to steam leak flow through valves and/or other connecting parts of the system ($\dot{Q}_L$) and the net heat loss rate ($\dot{Q}_{HL}$) through the whole outer surfaces of the system including the recirculation pumps. The net heat loss rate is given as

$$\dot{Q}_{HL} = \dot{Q}_C + \dot{Q}_B - \dot{Q}_L \ .$$

The test results of the heat loss tests are summarized in Table 3.2 and Fig. 3.3 and 3.4. $\dot{Q}_B$ and $\dot{Q}_L$ in the heat loss test results are estimated in chapter 4 and section 3.2. A simple relation between the net heat loss rate $\dot{Q}_{HL}$ and temperature difference ΔT between an average fluid temperature in the system T_F and the room temperature T_R has been obtained as

$$\dot{Q}_{HL} = 0.56 \times \Delta T \qquad (kJ/s)$$

$$\Delta T = T_F - T_R \qquad (°C) \ .$$

The average fluid temperature T_F in the system was obtained as a simple average value of the steam dome temperature (T-3) and the fluid temperature at break unit (T-19) shown in Table 3.1. Figure 3.4 shows the energy leakage rate $\dot{Q}_L$ is very small even at the highest saturation

temperature condition. On the other hand, the heat input from the recirculation pump $\dot{Q}_B$ contributes largely to heating the fluid, especially in the low saturation temperature conditions.

Figure 3.5 and 3.6 show the records of electric power supplied to the core at each heat loss test. These figures show the heating-up process and holding periods at each constant fluid temperature condition. Thermal steady condition was judged at stable electric power and then the heat loss test data were recorded.

3.2 Measurement of Steam Leakage Rate

Steam leakage rates in the heat loss tests and result of leakage test are presented below. The amount of steam leakage was detected by the water level change in the pressure vessel. In the heat loss tests, the water level change was recorded by DATAC 2000B system for 10 seconds and in all the heating-up and holding periods it was recorded by pen-recorder in the ROSA-III controlling system. The water level change during the holding period at each constant temperature condition are listed in Table 3.3. Mass leakage rate ($\dot{M}$) and corresponding energy leakage rate ($\dot{Q}_L$) was determined by using the volumetric change ΔV of the liquid water as

$$\dot{M} = \Delta V \times \gamma'/t$$

$$\dot{Q}_L = \Delta V \times (\gamma' h' - \gamma'' h'')/t \ ,$$

where γ' and γ'' are specific weights of saturated water and steam, h' and h'' are specific enthalpies of saturated water and steam and t is holding period. The mass leakage rate and the energy leakage rate at each holding period are also presented in the Table 3.3.

A leakage test was performed for one hour between the heat loss tests Case 6 and Case 7 in the same way as the heat loss tests. Figure 3.7 shows the data in the leakage test. The water level in the pressure vessel changed 118 mm in the DATAC 2000B recording system and it changed 114 mm in the pen-recorder of ROSA-III controlling system (See Table 3.3). This means that the indication of water level by the pen-recorder includes some error but the error is very small. The level change 118 mm means volumetric change of 0.045 m^3 as shown in Fig. 3.8. Test conditions of the leakage test and estimated values of both mass leakage rate

and corresponding energy leakage rate are summarized in Table 3.4 and 3.5, respectively. Figure 3.9 shows mass leakage rates and corresponding energy leakage rates due to steam leak flow.

Table 3.1 Test conditions of the heat loss tests

Measurements			Test Cases						
No.	Items	Units	1	2	3	4	5	6	7
1	Steam Dome Pressure	MPa	0.14	0.46	1.46	3.84	7.17	7.24	7.24
2	Steam Dome Temp. (T-3)(*)	°C	111	152	198	250	289	291	291
3	Temp. at Break B (T-19)	°C	110	151	196	248	286	288	288
4	Water Level in PV (WL-4)	m	4.569	4.852	4.767	5.238	5.275	5.484	5.355
5	Supplied Power (W-2)	kJ/s	29	53	80	114	134	145	136
6	Flow Rate of MRP-1 (F-27)	m^3/s	4.28×10^{-3}	4.38×10^{-3}	4.57×10^{-3}	4.72×10^{-3}	4.68×10^{-3}	4.75×10^{-3}	4.80×10^{-3}
7	Flow Rate of MRP-2 (F-28)	m^3/s	4.33 "	4.45 "	4.57 "	4.63 "	4.63 "	4.67 "	4.70 "
8	Pump Speed of MRP-1 (N-1)	rad./s	210	213	210	214	212	213	214
9	Pump Speed of MRP-2 (N-2)	rad./s	213	218	214	216	216	215	217
10	Pump Head of MRP-1 (D-14)	kPa	759	746	698	660	593	609	614
11	Pump Head of MRP-2 (D-15)	kPa	797	787	733	698	624	640	644
12	Room Temperature	°C	22.5	18.0	22.0	17.0	21.5	16.5	15.8

(*) Measurements with (sign) were recorded by DATAC 2000B system[1].

Table 3.2 Test results of the heat loss tests

$$\dot{Q}_{HL} = \dot{Q}_C + \dot{Q}_B - \dot{Q}_L$$

Items			Test Cases						
Sign.	Name	Units	1	2	3	4	5	6	7
P	Steam Dome Pressure	MPa	0.14	0.46	1.46	3.84	7.17	7.24	7.24
T_F	Average Fluid Temperature*	°C	110.5	151.5	197.0	249.0	287.5	289.5	289.5
T_R	Room Temperature	°C	22.5	18.0	22.0	17.0	21.5	16.5	15.8
ΔT	$\Delta T = T_F - T_R$	°C	88.0	133.5	175.0	232.0	266.0	273.0	273.7
$\dot{Q}_C$	Supplied Power	kJ/s	29	53	80	114	134	145	136
$\dot{Q}_B$	Heat Input from Pumps	kJ/s	25	24	23	21	19	19	19
$\dot{Q}_L$	Energy Leakage Rate	kJ/s	0.7	2.5	2.3	1.5	3.2	10.5	10.5
$\dot{Q}_{HL}$	Net Heat Loss Rate	kJ/s	53	74	101	133	150	153	144

* Average Fluid Temperature T_F is obtained as $\{(T\text{-}3) + (T\text{-}19)\} \times \frac{1}{2}$ shown in Table 3.1.

Table 3.3 Mass and energy leakage rates determined from water level change of pen-recorder data

Items	Units	Case 1	Case 2	Case 3	Case 4	Case 5	Leak Test
Steam Dome Pressure	MPa	0.14	0.46	1.46	3.84	7.17	7.24
Holding Periods	s	2280	2700	2160	1680	5220	3600
Initial Water Level	m	4.585	4.863	4.792	5.231	5.315	5.473
Final Water Level	m	4.572	4.833	4.767	5.223	5.263	5.359
Water Level Change	m	1.3×10^{-2}	3.0×10^{-2}	2.5×10^{-2}	8.0×10^{-3}	5.2×10^{-2}	1.14×10^{-1}
Volumetric Change ΔV	m^3	3.7×10^{-3}	1.2×10^{-2}	7.1×10^{-3}	2.3×10^{-3}	1.5×10^{-2}	4.4×10^{-2}
Mass Leakage Rate $\dot{M}$	kg/s	1.5×10^{-3}	3.9×10^{-3}	2.9×10^{-3}	1.4×10^{-3}	2.7×10^{-3}	8.5×10^{-3}
Energy Leakage Rate $\dot{Q}_L$	kJ/s	0.71	2.5	2.3	1.5	3.2	9.5

Table 3.4 Test conditions of leakage test

Measurements			Initial State	Final State
No.	Items	Units	$t = 0^H$	$t = 1^H$
1	Steam Dome Pressure	MPa	7.24	7.24
2	Steam Dome Temp. (T-3)(*)	°C	290	291
3	Temp. at Break B (T-19)	°C	288	288
4	Water Level in PV (WL-4)	m	5.473	5.355
5	Supplied Power (W-2)	kJ/s	148	136
6	Flow Rate at MRP-1 (F-27)	m^3/s	4.75×10^{-3}	4.80×10^{-3}
7	Flow Rate at MRP-2 (F-28)	m^3/s	4.67×10^{-3}	4.70×10^{-3}
8	Pump Speed of MRP-1 (N-1)	rad./s	213	214
9	Pump Speed of MRP-2 (N-2)	rad./s	218	217
10	Room Temperature	°C	16.5	15.8
11	Water Level in PV(**)	m	5.473	5.359

(*) Measurement with (sign) were recorded by DATAC 2000B system[1].

(**) Data from the pen-recorder

Table 3.5 Mass and energy leakage rates in the leakage test

Items	Units	Values
Steam Dome Pressure	MPa	7.24
Holding Periods	s	3600
Water Level Change(*)	m	1.18×10^{-1}
Volumetric Change ΔV	m^3	4.5×10^{-2}
Mass Leakage Rate $\dot{M}$	kg/s	8.9×10^{-3}
Energy Leakage Rate $\dot{Q}_L$	kJ/s	10.5

(*) Datum by DATAC 2000B recording system

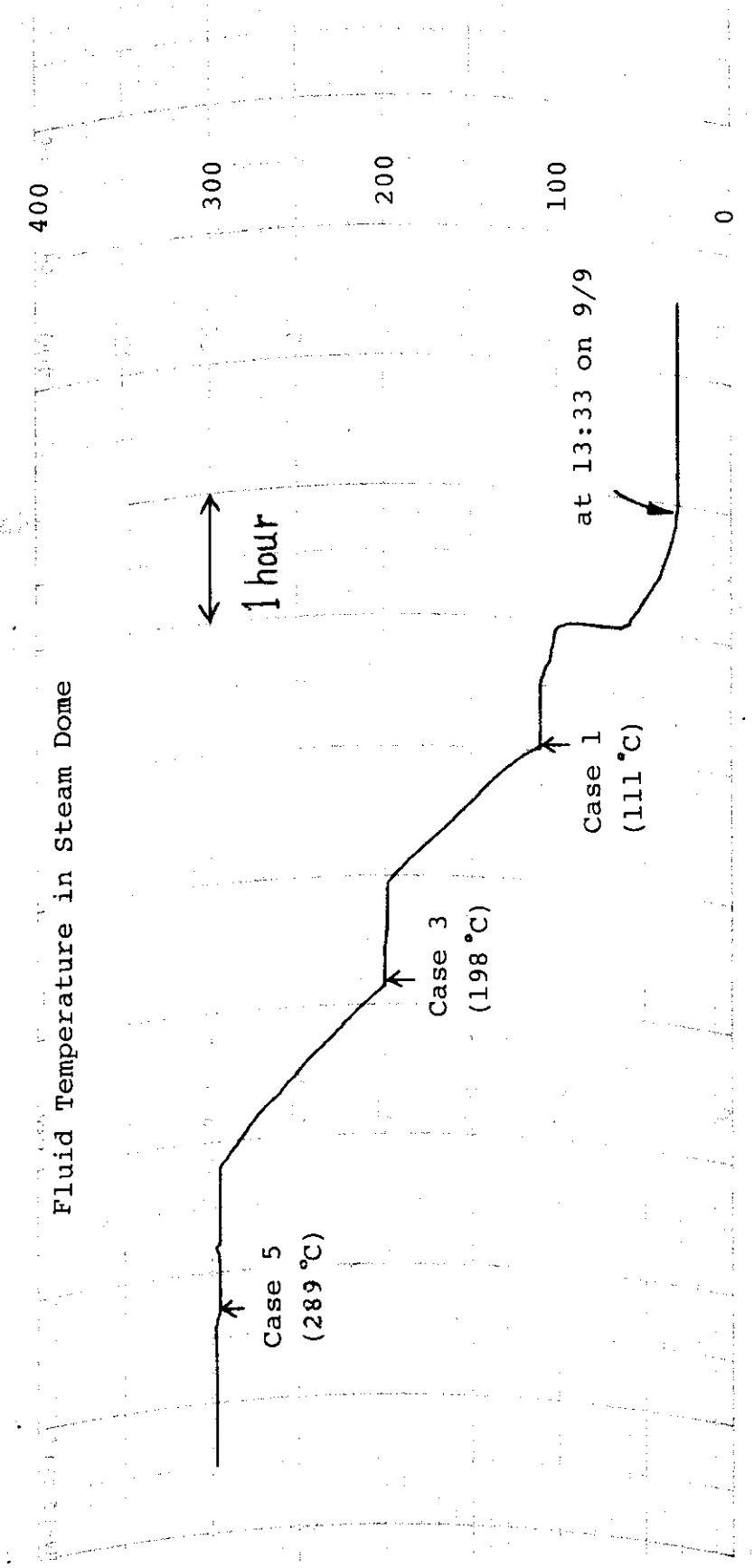

Fig. 3.1 Temperature history recorded during heat loss tests (Case 1, 3, 5)

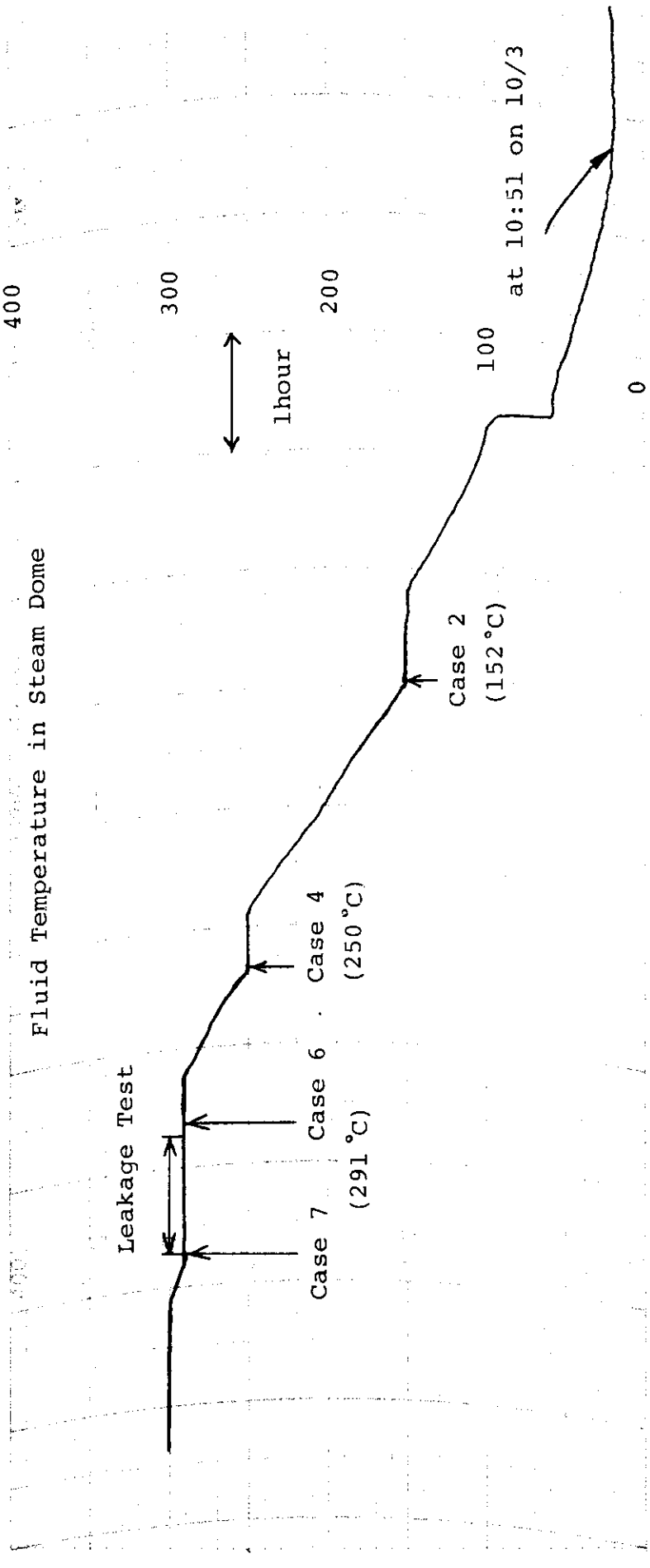

Fig. 3.2 Temperature history recorded during heat loss tests (Case 2, 4, 6, 7)

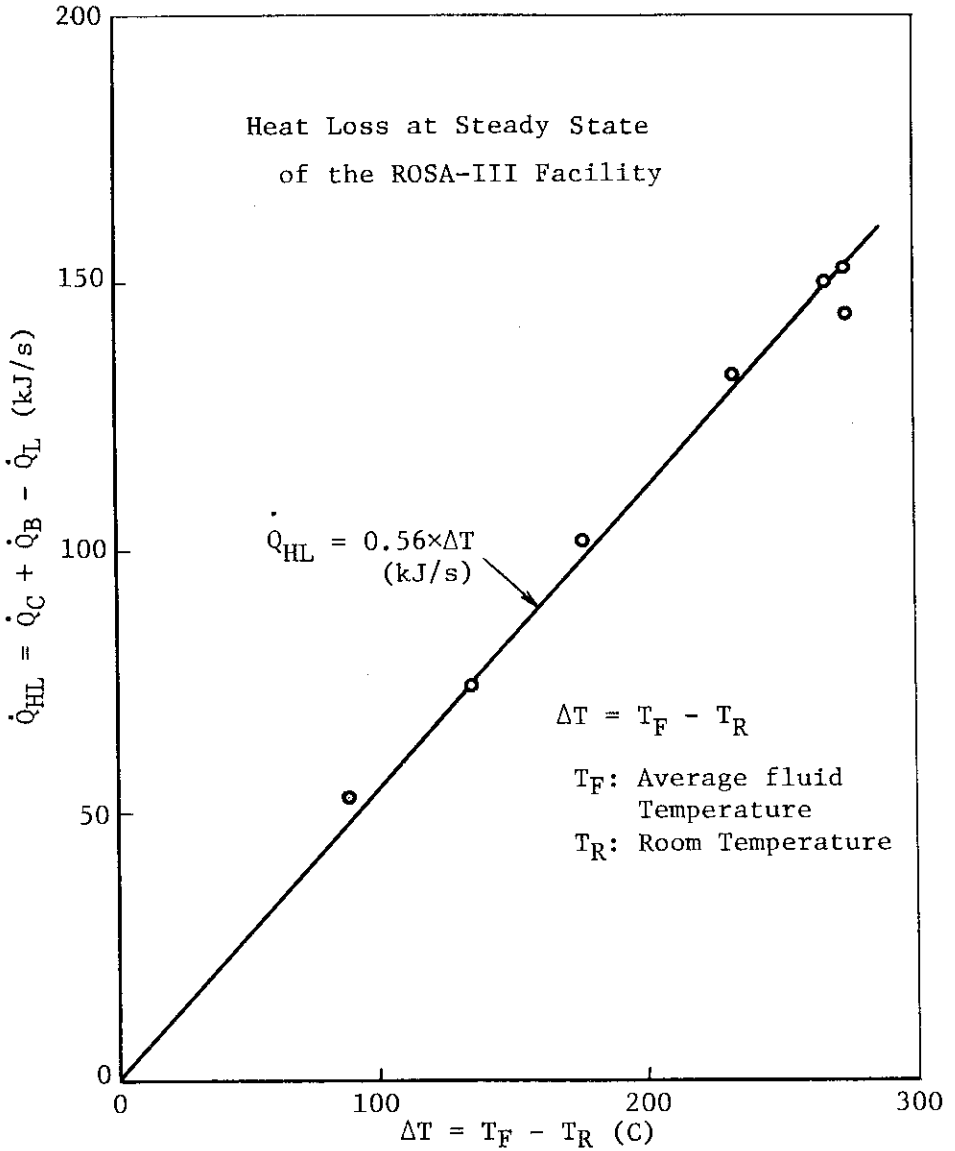

Fig. 3.3 Relation between the net heat loss rate and the temperature difference between fluid temperature in the system and the room temperature

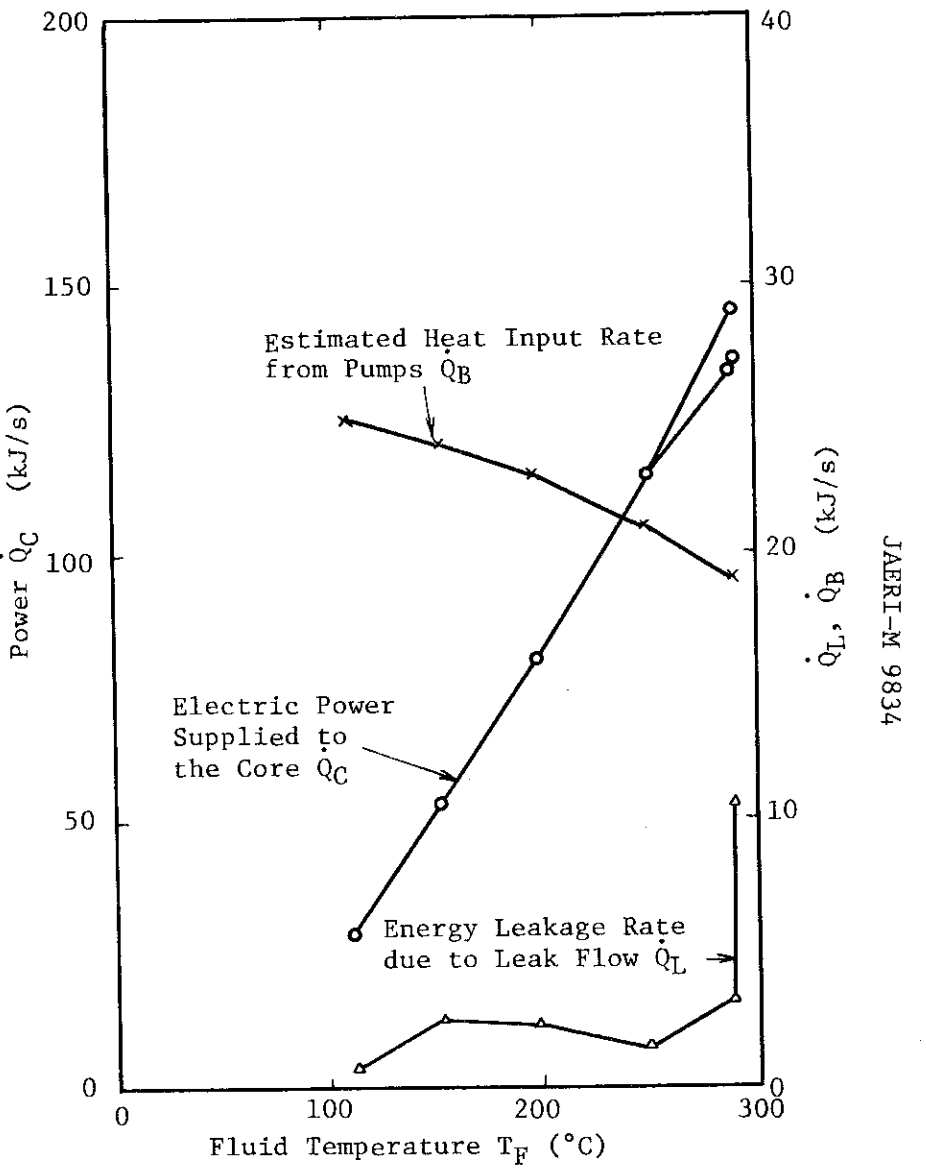

Fig. 3.4 Electric power in the core $\dot{Q}_C$, heat input rate from the pumps $\dot{Q}_B$ and energy leakage rate $\dot{Q}_L$ in the heat loss and leakage tests

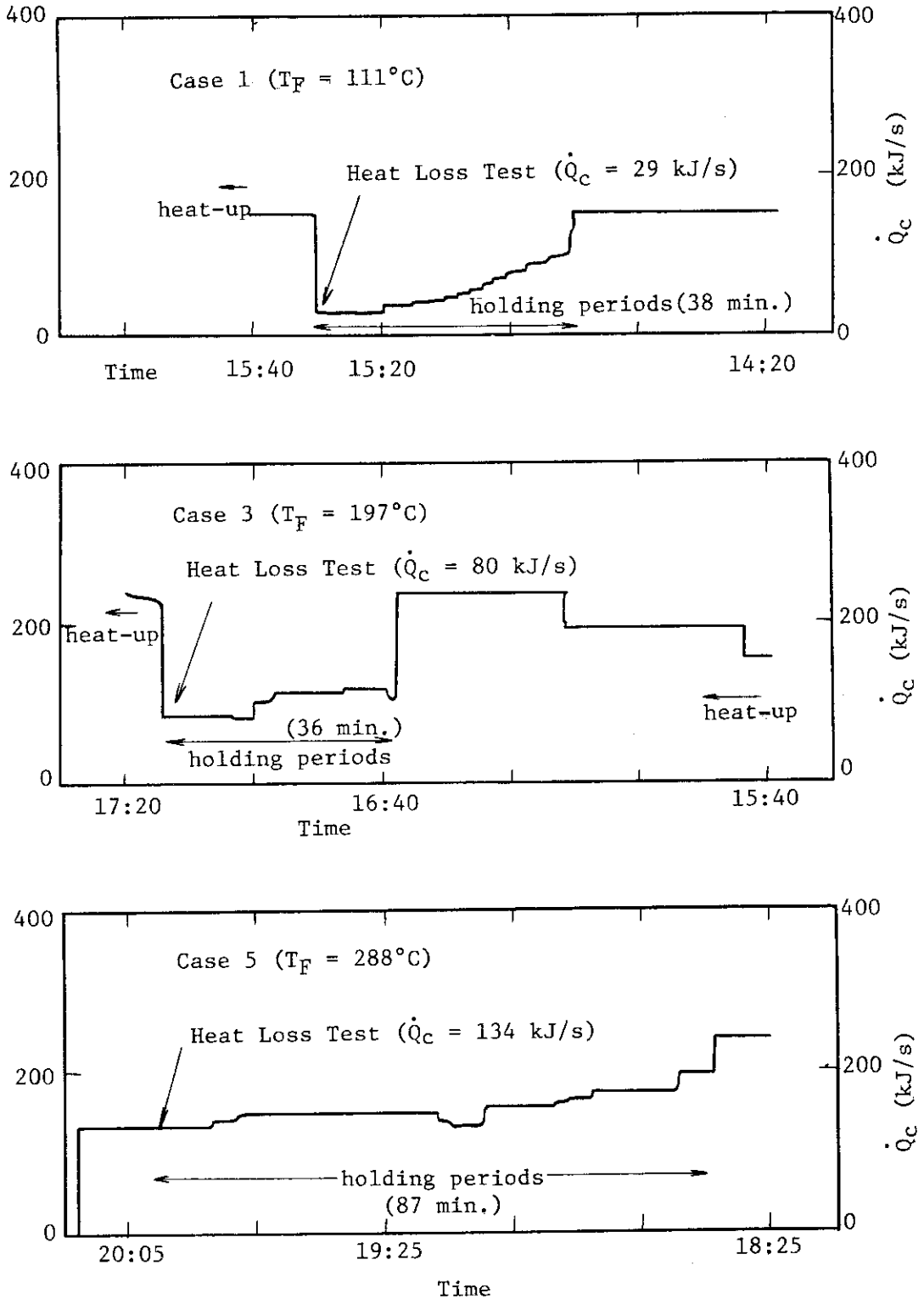

Fig. 3.5 Electric power supplied to the core in the heating-up and holding periods (Case 1, 3, 5)

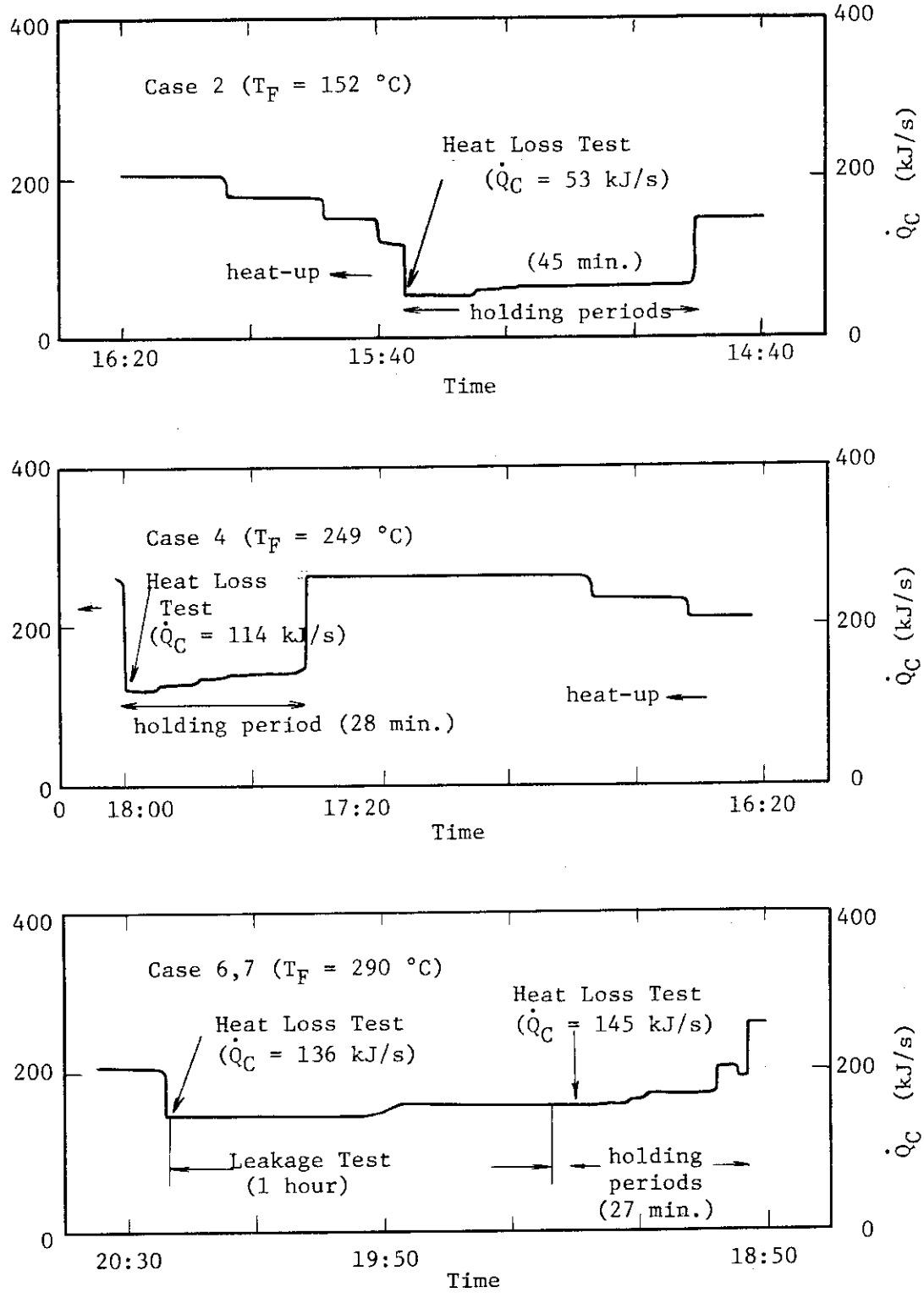

Fig. 3.6 Electric power supplied to the core in the heating-up and holding periods (Case 2, 4, 6, 7)

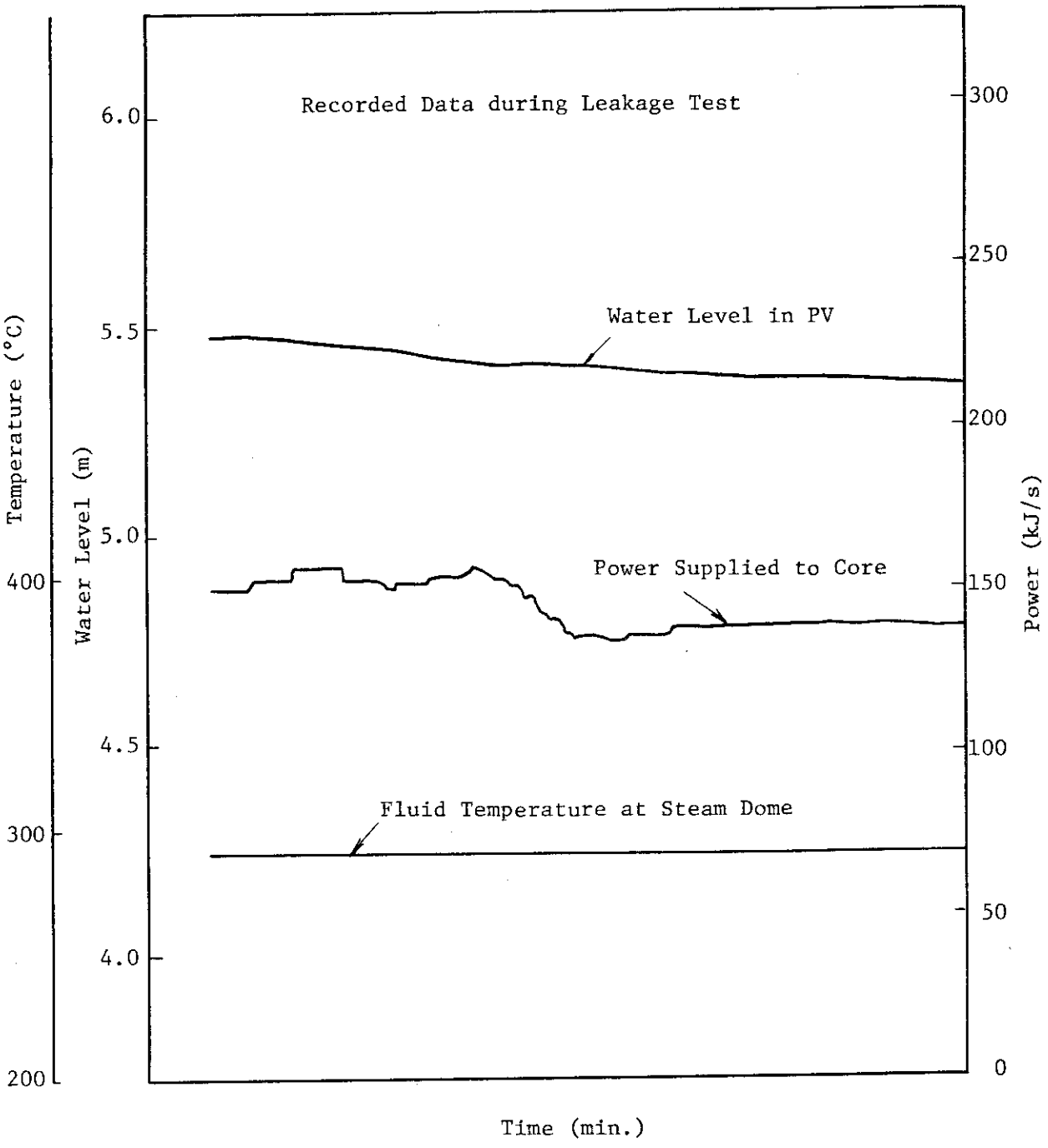

Fig. 3.7 PV water level, steam dome temperature and power supplied to the core during the leakage test

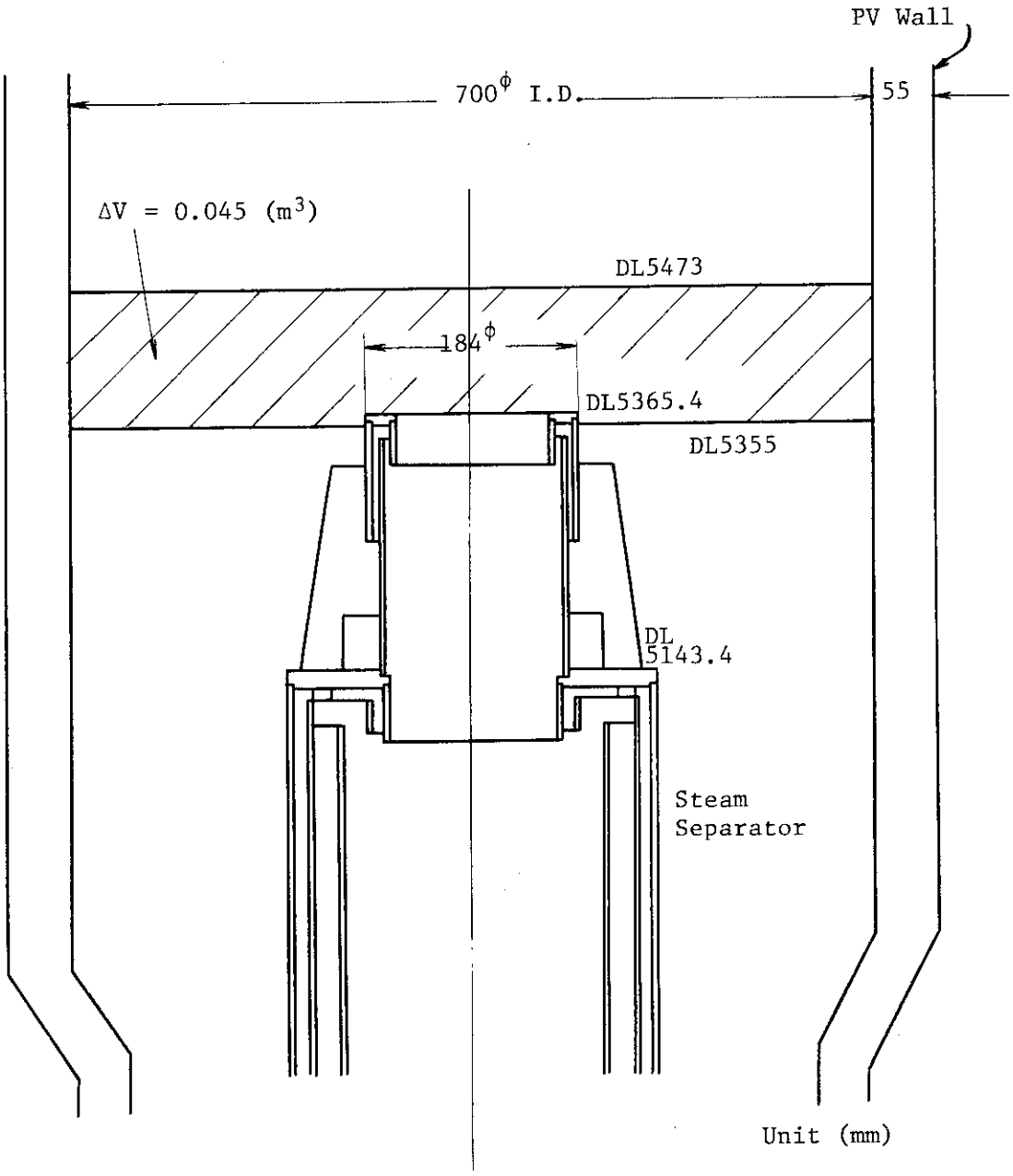

Fig. 3.8 Internal structure of the pressure vessel at the vicinity of water level in the leakage test

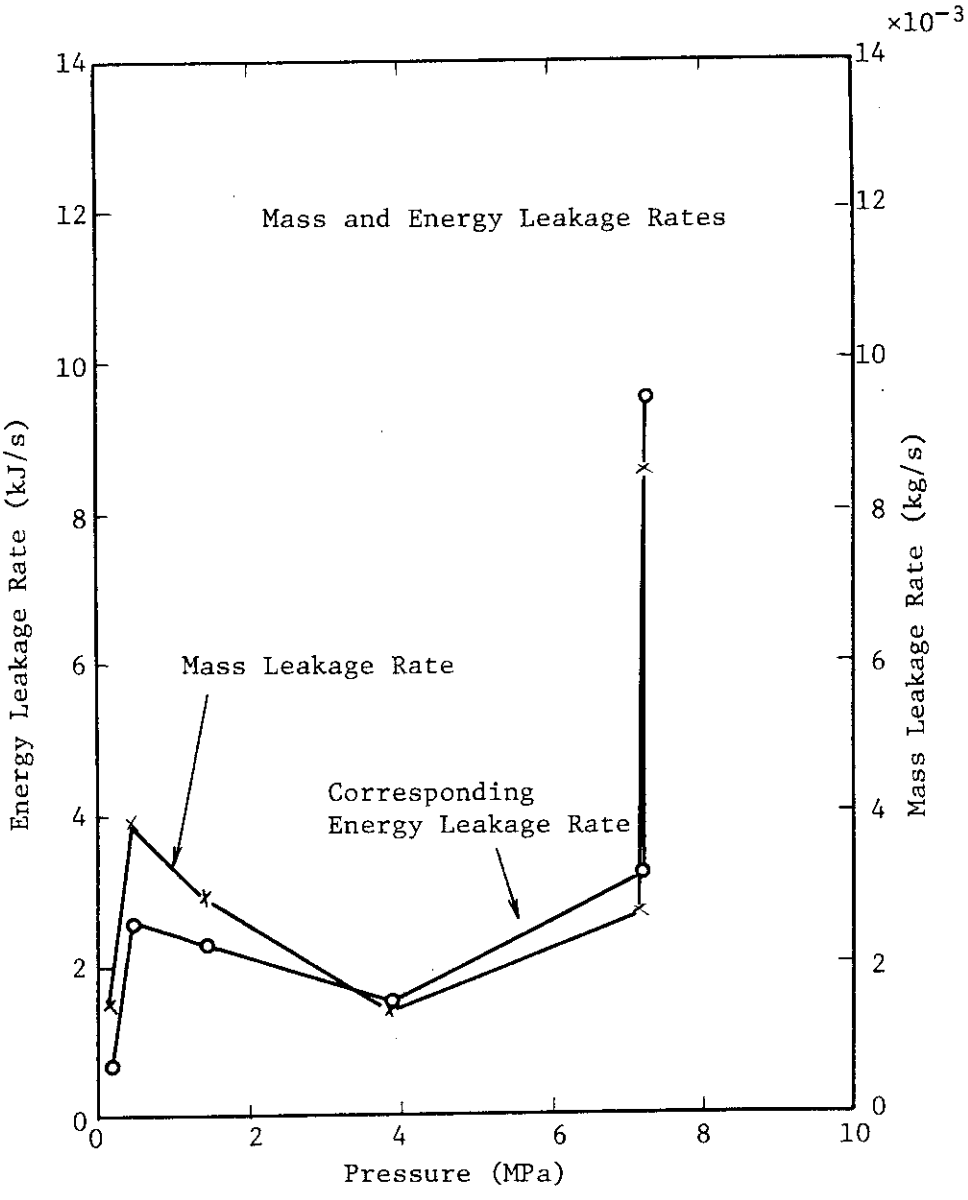

Fig. 3.9 Mass and energy leakage rates during the heat loss and leakage tests

4. Estimation of Heat Input from the Pumps

Heat input from the operating recirculation pumps was not obtained directly using the electric power supplied to the motor and carried energy by the cooling water because of the inaccurate measurements of flow rate and temperature difference of the cooling water passed through the pump motor. The heat input from the operating pumps was estimated indirectly as follows.

Brake horse power given to a pump from a motor $\dot{Q}_B$ changes to hydraulic power $\dot{Q}_H$ and pump frictional power $\dot{Q}_F$. A pump efficiency (η_p) is given by

$$\eta_p = \dot{Q}_H \,/\, \dot{Q}_B \quad ,$$

$$\dot{Q}_B = \dot{Q}_H + \dot{Q}_F \quad .$$

And the hydraulic power is expressed as

$$\dot{Q}_H = \gamma Q H \,/\, 102 \qquad (kJ/s)$$

where γ : specific weight (kgf/m^3)
Q : volumetric flow rate (m^3/s)
H : pump head (m).

All the hydraulic power $\dot{Q}_H$ becomes a heat input to the fluid in the system. On the other hand, a part of the friction power $\dot{Q}_F$ generated in the pump is transported to outside of the pump by heat conduction and other part of it contributes to heat up the fluid in the system. The heat loss through the pump outer surface, however, is a part of the whole heat loss through all pressure boundary of the ROSA-III test facility. Therefore, all brake horse power given to the pump can be regarded as heat input to the fluid in the case of these heat loss tests.

The brake horse power[5] of the ROSA-III recirculation pumps has been determined by using a relation between the theoretical pump efficiency η_{th} and the hydraulic power $\dot{Q}_H$ as

$$\dot{Q}_B = \dot{Q}_H \,/\, \eta_{th} \quad .$$

The heat input from the operating recirculation pumps in the heat loss and leakage tests was determined by using above pump data and by assuming

a proportionality of the brake horse power as to fluid density in the system. The heat input from the pumps at consta speed 213 rad./s (2030 rpm), volumetric flow rate 4.33×10^{-3} m^3/s (260 ℓ/min) and arbitrary fluid specific weight $\gamma(kgf/m^3)$ is given as

$$\dot{Q}_B = 2Q_{BO} \times (\gamma/\gamma_0)$$

where $\dot{Q}_{BO}$: brake horse power per one pump at 25°C fluid temperature

γ_0 : specific weight of fluid at 25°C.

$\dot{Q}_{BO}$ was determined from Fig. 4.1(a) as 13 kJ/s per one pump. Figure 4.1(b) and 4.2 show the brake horse power and the hydraulic power characteristics. The heat input from the pumps at each heat loss tests and leakage test are summarized in Table 4.1.

Table 4.1 Heat input from the recirculation pumps $\dot{Q}_B$

Items	Units	Case 1	Case 2	Case 3	Case 4	Case 5	Case 6	Case 7
Steam Dome Pressure	MPa	0.14	0.46	1.46	3.84	7.17	7.24	7.24
Fluid Specific Weight	kgf/m^3	951	918	868	802	737	735	735
Heat Input $\dot{Q}_B$	kJ/s	25	24	23	21	19	19	19

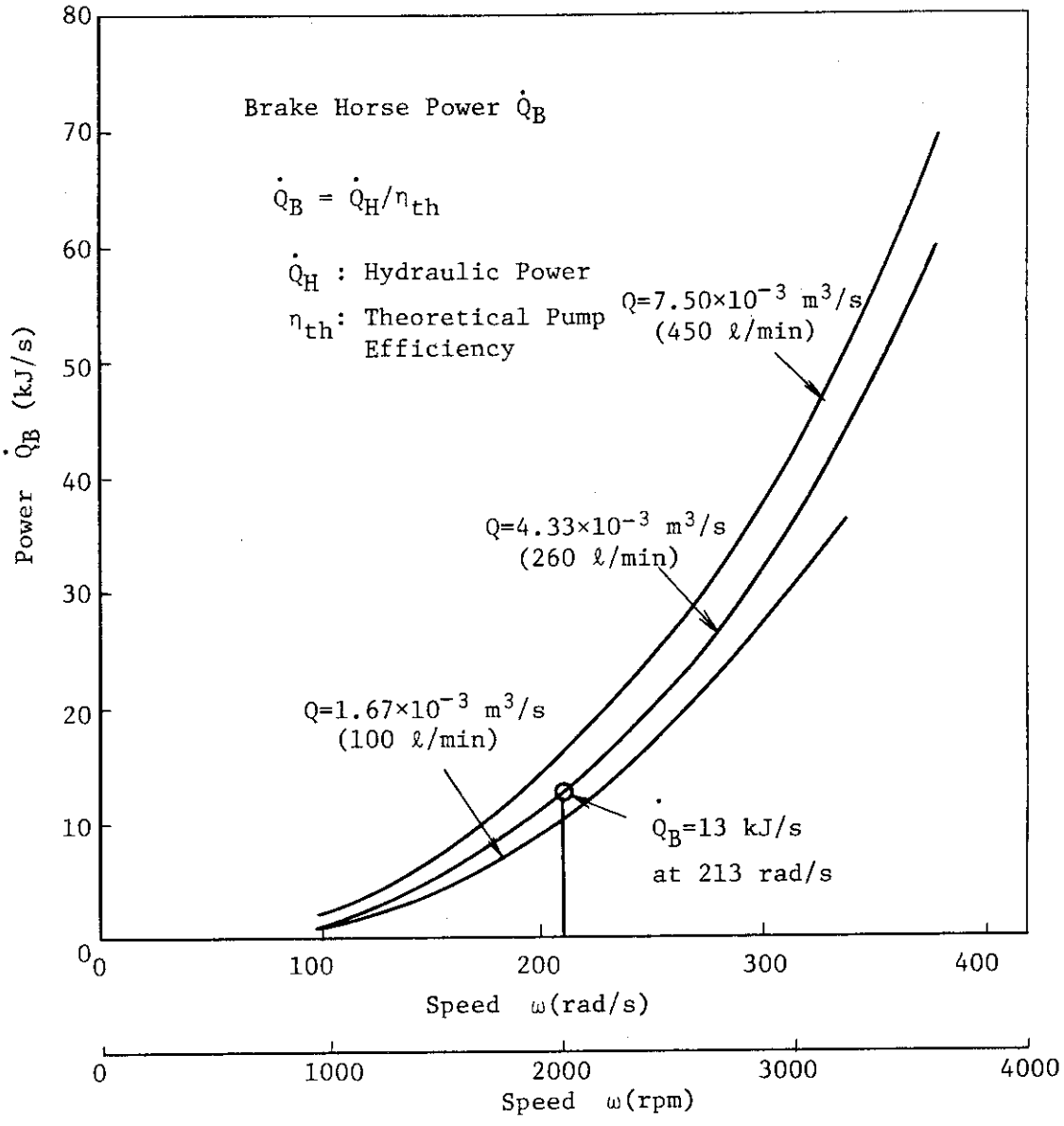

Fig. 4.1(a) Brake horse power supplied to the MRP-1 pump with flow parameter (Fluid Temperature 25 °C)

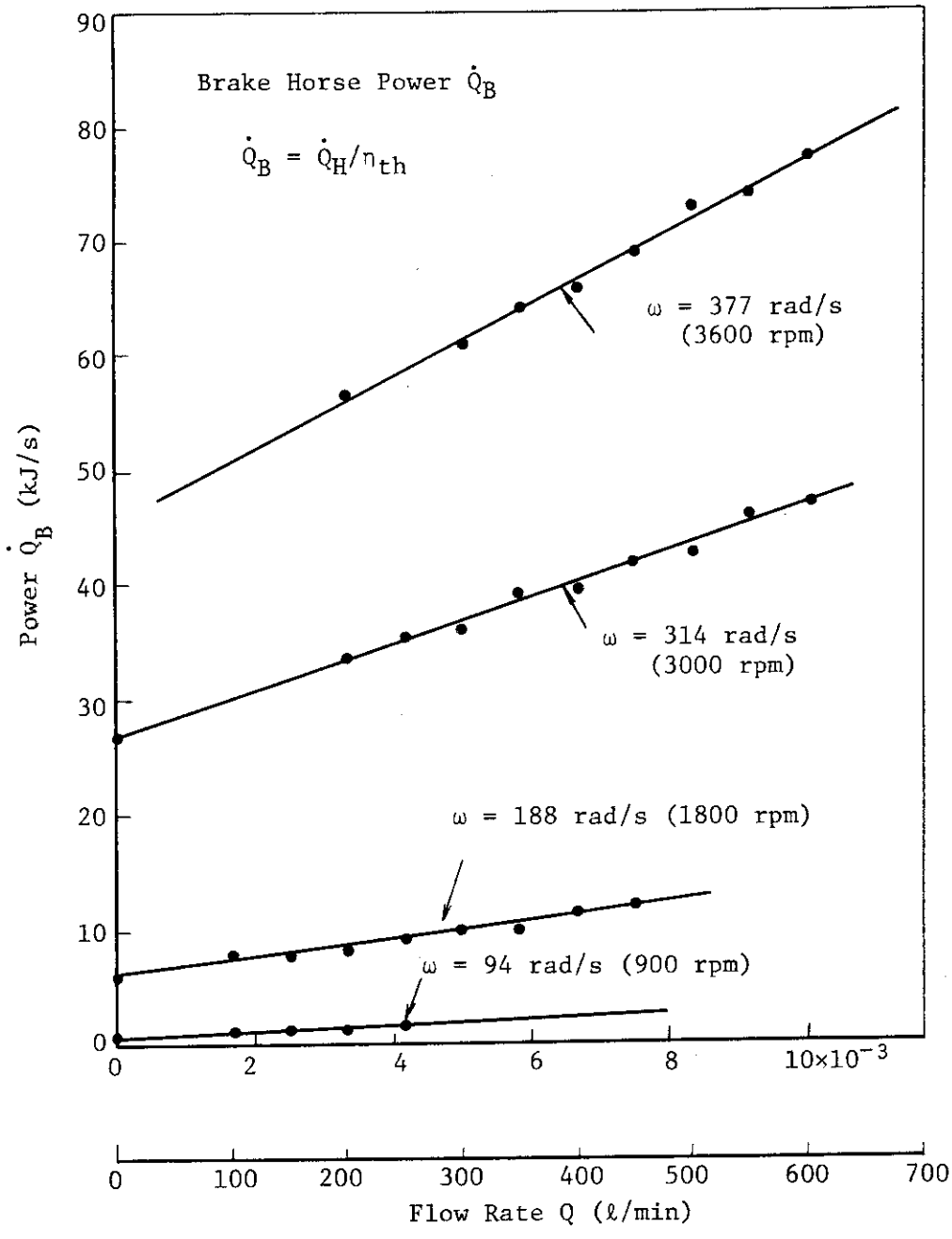

Fig. 4.1(b) Brake horse power supplied to the MRP-1 pump with pump speed parameter (Fluid Temperature 25 °C)

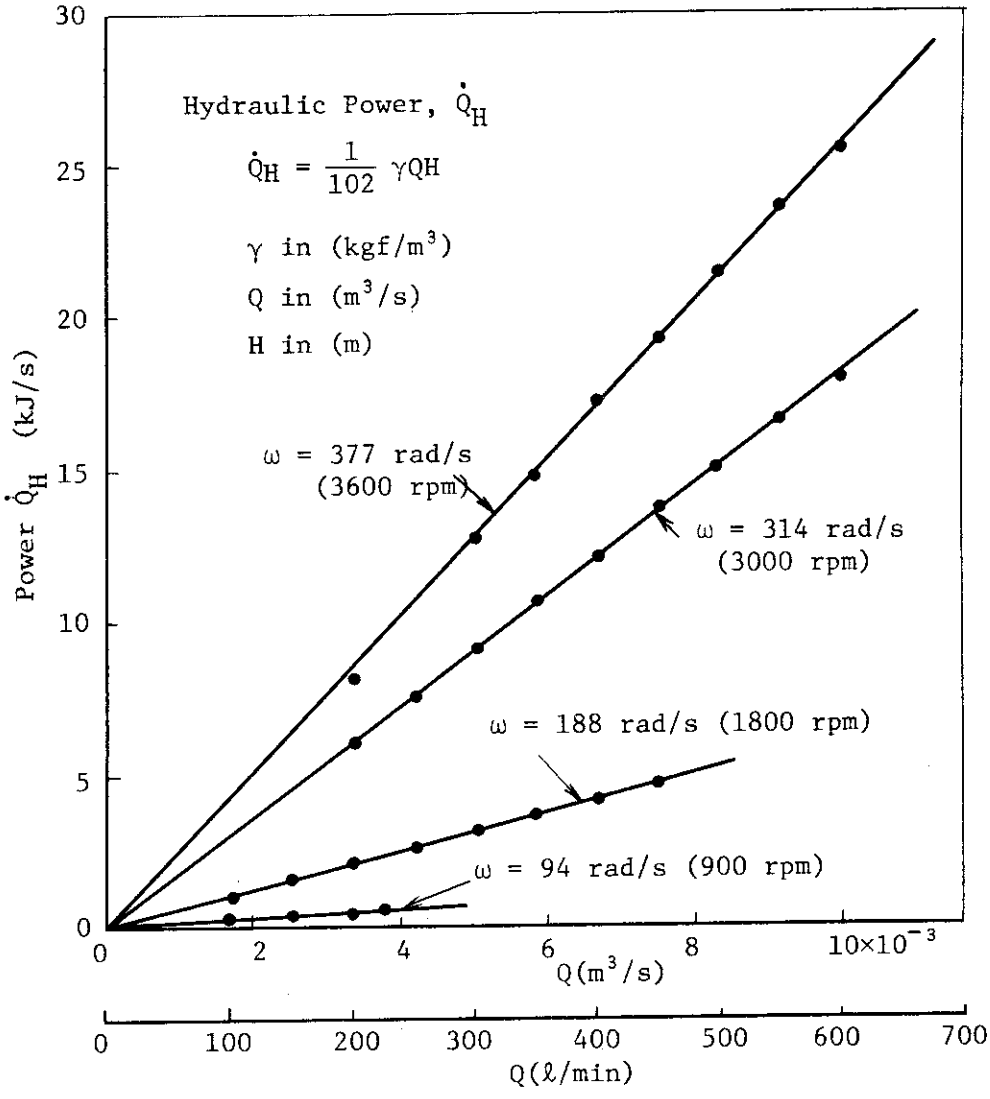

Fig. 4.2 Hydraulic power of the MRP-1 pump

5. Discussions of Test Results

Thermal steady state in the heat loss tests and the leakage test, and the average surface heat flux corresponding to the heat loss are discussed in the present section.

(1) Approximation of the Thermal Steady State

For establishing the thermal steady state of the fluid system, the thickness of the metal walls surrounding the coolant have a dominating effect. Representative wall thickness of the recirculation loops and the pressure vessel are 5.5 mm for the former pipings (2B, Sch 80), 40 mm for the downcomer wall, 130 mm for the average pressure vessel wall and 210 mm for the top part of the pressure vessel. As shown in Appendix A, most of structural materials made of SUS 304 with one-side insulation become thermally steady condition in one hour after stepwise temperature change at the heating surface. Quasi-steady condition (difined as η value more than 0.9 in Fig. A.3) can be established after 2.6 hours even for the extreme thick walls such as the 210 mm walls. The similar thick metal parts exist at the flanges connecting the upper and the lower main part of the pressure vessel, the bottom flange of the pressure vessel and the two recirculation pumps in the loops. Unsolved problems in the discussions of thermally steady state exist in the imperfect insulation conditions at the outer surfaces and in the sequential heating-up process which is different from the stepside temperature increase at one side of the wall. These are not estimated analytically but experimentally.

In the case of heat loss tests, it took more than 4 hours for heating up the fluid in the ROSA-III system from 100°C to 290°C and took more than 27 minutes for confirming the thermal steady state by the stable core heat generation before the data aquisition by DATAC 2000 B system. Figures 3.5 and 3.6 show transient values of the electric power supplied to the core. The fluid system was maintained at the constant pressure during the holding period in each heat loss test. In the tests of Case 1, 2, 3 and 5, the core power maintained constant more than 8 minutes before the data aquisition. It is considered empirically that stable core power for 8 minutes shows establishment of approximate thermal steady state condition in the system. In the tests of Case 4 and 6, however, periods of stable core power are 4 and 3 minutes, respectively. These periods are rather short comparing with those of other cases.

The short holding period in the Case 6 caused higher core power than that in the Case 7 conducted about one hour after the Case 6. Figure 3.7 shows that fluid condition in the Case 7 was nearly steady state. The difference of core power between Case 6 and 7, 9 kJ/s (6% of net heat loss rate at $\Delta T = 270°C$), can be considered as a maximum error in the heat loss tests. It is concluded that thermal steady condition was approximately established in each heat loss test and that estimated net heat loss rate may include a measuring error, 6%.

(2) Average surface heat flux due to the heat loss

Approximate inner surface areas of the pressure vessel and the recirculation loops are 12.4 m^2 and 11.3 m^2, respectively. Average surface heat flux due to heat loss at the operating conditions of the ROSA-III test (P = 7.3 MPa, T_F = 289°C) can be estimated for the following cases.

(a) Heat releases only through the pressure vessel wall (area : A = 12.4 m^2)

(b) Heat release through the pressure vessel and the recirculation loops walls (area : A = 23.7 m^2)

The heat loss rate at the fluid condition is given from Fig. 3.3 by assuming a room temperature 20°C as

$$\dot{Q}_{HL} = 151 \quad (kJ/s)$$

$$= 1.30 \times 10^5 \quad (kcal/hr) \quad .$$

Therefore, the average surface heat fluxes (q) due to heat loss in two cases are determined as

(a) $q \equiv \dot{Q}_{HL} / A = 12.2\ kJ/m^2 \cdot s$

$$= 1.05 \times 10^4 \quad kca./m^2 \cdot hr$$

(b) $q = 6.37\ kJ/m^2 \cdot s$

$$= 5.49 \times 10^3\ kcal/m^2 \cdot hr$$

6. Conclusions

The heat loss rates and the steam leakage rates at five different fluid conditions of the ROSA-III test facility have been measured taking into account the heat input from the operating recirculation pumps and the energy leakage due to steam leak flow.

(a) The net heat loss rate $\dot{Q}_{HL}$ in the ROSA-III facility is proportional to the temperature difference ΔT between the fluid temperature in the system and the room temperature as

$$\dot{Q}_{HL} = 0.56 \times \Delta T \qquad (kJ/s)$$

where ΔT is in the unit of °C. Measurement error is included about 6% of the net heat loss rate.

(b) The mass leakage rate $\dot{M}$ of the ROSA-III test at pressure 7.24 MPa was measured as 8.9×10^{-3} kg/s, which corresponded to energy leakage rate of 10.5 kJ/s.

(c) Contribution of heat input from the operating pumps to the heat balance of the fluid system was fairly large comparing with the effect of fluid leakage.

(d) Average heat fluxes (q) due to the heat loss through the pressure boundary walls were estimated at the operating conditions of the ROSA-III test (P = 7.3 MPa, T = 289°C) as

1° $q = 12.2$ kJ/m^2·s : heat loss through only PV walls

2° $q = 6.4$ kJ/m^2·s : heat loss through PV and loop walls.

Acknowledgment

The authors wish to express their appreciation to Mr. T. Fujishiro of Reactivity Accident Laboratory for his precise comments and advices and to H. Murata of Reactor Safety Laboratory 1 in JAERI and to H. Asahi and other members of Nuclear Engineering Co. for their conducting the heat loss tests and the leakage test.

6. Conclusions

The heat loss rates and the steam leakage rates at five different fluid conditions of the ROSA-III test facility have been measured taking into account the heat input from the operating recirculation pumps and the energy leakage due to steam leak flow.

(a) The net heat loss rate $\dot{Q}_{HL}$ in the ROSA-III facility is proportional to the temperature difference ΔT between the fluid temperature in the system and the room temperature as

$$\dot{Q}_{HL} = 0.56 \times \Delta T \qquad (kJ/s)$$

where ΔT is in the unit of °C. Measurement error is included about 6% of the net heat loss rate.

(b) The mass leakage rate $\dot{M}$ of the ROSA-III test at pressure 7.24 MPa was measured as 8.9×10^{-3} kg/s, which corresponded to energy leakage rate of 10.5 kJ/s.

(c) Contribution of heat input from the operating pumps to the heat balance of the fluid system was fairly large comparing with the effect of fluid leakage.

(d) Average heat fluxes (q) due to the heat loss through the pressure boundary walls were estimated at the operating conditions of the ROSA-III test (P = 7.3 MPa, T = 289°C) as

1° $q = 12.2$ kJ/m^2·s : heat loss through only PV walls

2° $q = 6.4$ kJ/m^2·s : heat loss through PV and loop walls.

Acknowledgment

The authors wish to express their appreciation to Mr. T. Fujishiro of Reactivity Accident Laboratory for his precise comments and advices and to H. Murata of Reactor Safety Laboratory 1 in JAERI and to H. Asahi and other members of Nuclear Engineering Co. for their conducting the heat loss tests and the leakage test.

References

(1) Y. Anoda, et al., "ROSA-III System Description for Fuel Assembly No.4", JAERI-M 9363, February (1981).

(2) M. Suzuki, et al., "Characteristics of the ROSA-III Test Facility (Characteristics Test of the Jet Pumps in Normal and Reverse Flow)', JAERI-M 8670, February (1980).

(3) H. Kumamaru, et al., "Relation between Liquid Level Signal Obtained by ROSA-III Type Conductivity Probe and Liquid Level, Flow Pattern or Void Fraction", JAERI-M 9307, February (1981).

(4) M. Suzuki, et al., "Single Phase Pump Head Characteristics of Recirculation Pumps of the ROSA-III Facility", to be published.

(5) A Report of Inspection Test Results on the ROSA-III Facility Vol.I, Chap.8, "NIKKISO Non-seal Pump Test Records", Sumitomo Heavy Industries, LTD., March (1978).

Appendix A

Transient Temperature Profile in Thick Metal Walls with One-side Insulation

One dimensional heat conduction problem is solved analytically to clarify a time period necessary to arrive at thermal quasi-steady state in the ROSA-III facility. As most of metal walls of the pressure vessel and the recirculation pipings are surrounded by the insulator made of glass wool, the metal walls are assumed to be insulated well. The cylindrical walls of the pressure vessel are assumed to be flat plate.

A flat plate with thickness ℓ is assumed as shown in Fig. A.1. One dimensional heat conduction problem in a flat plate with thickness $\frac{\ell}{2}$ and with one-side insulation is equivalent to that problem with thickness ℓ and with the same thermal conditions on both surfaces. The plate is initially maintained at constant temperature T_0 (°C) and suddenly both surfaces are heated up and maintained to a temperature T_1 (°C). Basic equation and analytical conditions for this case are shown as follows by using non-dimensional temperature $\theta = (T_1 - T)/(T_1 - T_0)$ and a constant thermal diffusivity K (m^2/s),

$$\frac{\partial \theta}{\partial t} = K \frac{\partial^2 \theta}{\partial x^2} \tag{A.1}$$

and

$$\theta = 1 \quad \text{at} \quad t = 0 \tag{A.2}$$

$$\theta = 0 \quad \text{at} \quad x = 0, \ \ell \ . \tag{A.3}$$

The equation (A.1) is solved easily by using a function of distance X(x) and time Y(t), namely

$$\theta = X(x) \times Y(t) \quad , \tag{A.4}$$

and differential equations for X(x) and Y(t) are given by using a

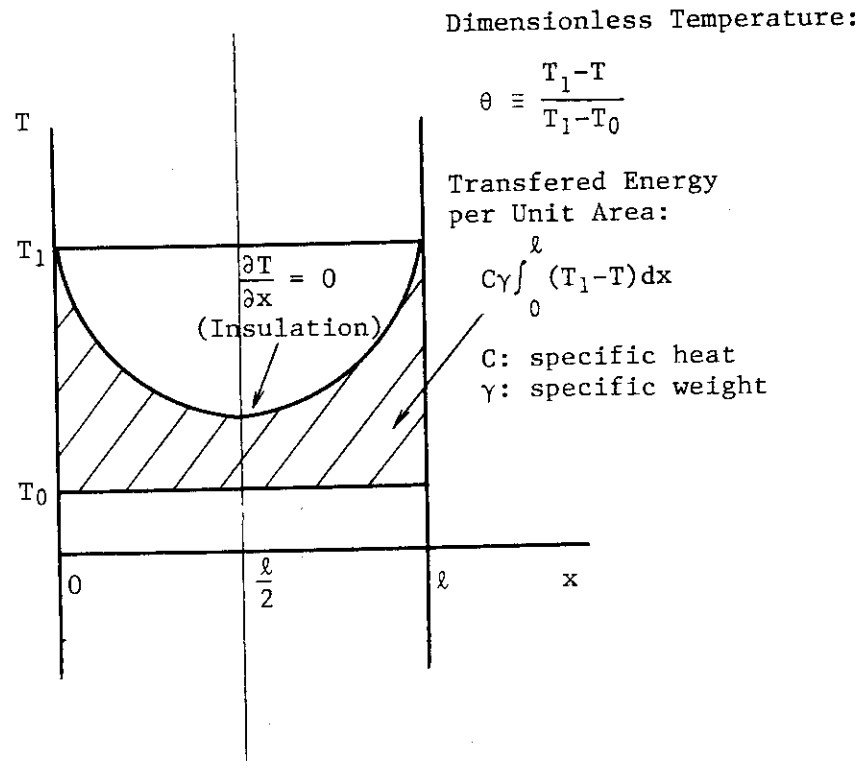

Fig. A.1 One-dimensional heat conduction model through a wide flat plate with sudden temperature rise at both surfaces

constant P^2, as

$$\frac{dY}{Y} = -KP^2dt \tag{A.5}$$

$$\frac{d^2X}{dx^2} + P^2X = 0 \ . \tag{A.6}$$

Therefore X(x) and Y(t) are expressed as

$$X(x) = A \sin Px + B \cos Px \tag{A.7}$$

$$Y(t) = e^{-KP^2t} \tag{A.8}$$

where P, A and B are constants determined from analytical conditions. By using an analytical condition (A.3) on equation (A.7),

$$B = 0 \tag{A.9}$$

$$\left.\begin{aligned} &\sin P\ell = 0 \\ &Pn = \frac{n\pi}{\ell} \quad (n=1,\ 2,\ 3,\ 4,\ \text{-----}) \end{aligned}\right\} \tag{A.10}$$

are obtained and X(x) and Y(t) are described corresponding to each eigenvalue Pn, as

$$Xn(x) = An \sin Pn\ x \tag{A.11}$$

$$Yn(t) = e^{-KPn^2t} \ . \tag{A.12}$$

Therefore a general solution is given as a linear combination of Xn(x) Yn(t), namely

$$\theta = \sum_{n=1}^{\infty} An\ e^{-KPn^2t} \times \sin Pn\ x \tag{A.13}$$

By using the analytical condition (A.2) to the equation (A.13),

$$1 = \sum_{n=1}^{\infty} An \sin Pn\ x \tag{A.14}$$

is obtained. The constants An are determined by an orthogonality relation of the eigenfunction sin Pn x as

$$\int_0^{\ell} \sin Pn\ x \times \sin Pm\ x \ dx$$

$$\begin{cases} = 0 & \text{for} \quad n \neq m \\ = 1 & \text{for} \quad n = m \ , \end{cases} \tag{A.15}$$

therefore

$$\left.\begin{aligned} An &= \frac{4}{n\pi} \qquad \text{for} \quad n = 1,\ 3,\ 5,\ 7,\ \text{---} \\ &= 0 \qquad \text{for} \quad n = 2,\ 4,\ 6,\ 8,\ \text{---} \end{aligned}\right\} \tag{A.16}$$

Concludingly the dimensionless temperature θ is expressed as,

$$\theta = \sum_{n} \frac{4}{n\pi} e^{-\frac{(n\pi)^2Kt}{\ell^2}} \times \sin \frac{n\pi x}{\ell} \tag{A.17}$$

$$(n = 1,\ 3,\ 5,\ 7,\ \text{---}\ ).$$

Table A.1 Non-dimensional temperature θ in the case of sudden temperature rise at both surfaces of wide flat plate

$$\theta(x, t) = \sum_n \frac{4}{n\pi} e^{-F(n\pi)^2} \sin \frac{n\pi x}{\ell}$$

$$F = Kt/\ell^2$$

Fourier No.	Distance from Surface x/ℓ						
F	0.05	0.10	0.15	0.20	0.30	0.40	0.50
0.001	0.813	0.967	1.004	—	—	—	—
0.01	0.276	0.521	0.711	0.843	0.966	0.995	0.999
0.05	0.124	0.244	0.358	0.462	0.630	0.736	0.772
0.10	0.074	0.147	0.215	0.279	0.384	0.451	0.475
0.20	0.028	0.055	0.080	0.104	0.143	0.168	0.177
0.50	0.001	0.003	0.004	0.005	0.007	0.008	0.009
1.00	1.0×10^{-5}	2.0×10^{-5}	3.0×10^{-5}	3.9×10^{-5}	5.3×10^{-5}	6.3×10^{-5}	6.6×10^{-5}

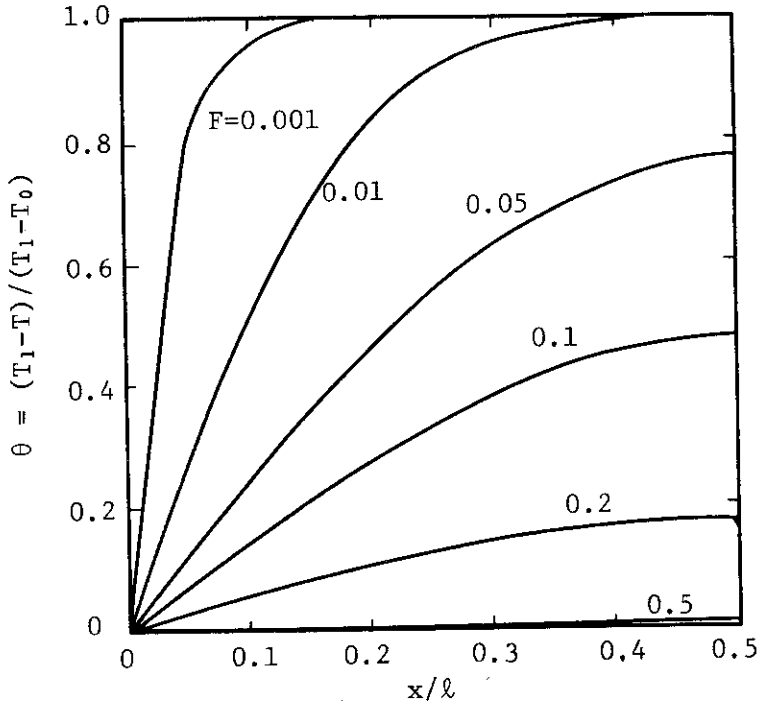

Fig. A.2 Non-dimensional temperature profile in the case of sudden temperature rise at both surfaces of a wide flat plate

($F = kt/\ell^2$: Fourier Number, ℓ: plate thickness)

This temperature is described by two non-dimensional parameter Kt/ℓ^2, a Fourier number and x/ℓ, a non-dimensional distance as shown in Table A.1 and Fig. A.2. In the case of wall with one-side insulation, distance x may be taken as $0 \leq x \leq \ell/2$ and the insulation condition

$$\left.\frac{\partial\theta}{\partial x}\right|_{x=\frac{\ell}{2}} = 0 \tag{A.18}$$

is satisfied in the equation (A.17).

A simple factor is necessary for indicating the degree of approximation to the perfect thermal equilibrium state in the case of sudden temperature change at one surface wall and insulation at the other surface. A degree of approximation η to thermally steady state is defined from a heat capacity ratio between heat capacity increased from initial state to time t and that to time infinity, namely

$$\eta \equiv \frac{1}{\ell}\int_0^{\ell}(1-\theta)\,dx$$

$$= 1 - \sum_n \frac{8}{(n\pi)^2} e^{-\frac{(n\pi)^2 Kt}{\ell^2}} \tag{A.19}$$

$$(n = 1, 3, 5, 7, \text{---}\ ).$$

The value η is shown in the cases of representative walls of the ROSA-III facility made of SUS 304 steel with wall thickness $\frac{\ell}{2}$ = 5.5, 40, 130 and 210 (mm) by using the Fourier number F as a parameter in Table A.2 and Fig. A.3.

It is shown from these results that the metal walls with thickness less than 40 mm become nearly thermal equilibrium condition in 30 minutes. And after 2.6 hours, the increased heat capacity becomes 90% of final heat capacity in the most thick wall of the pressure vessel with thickness 210 mm.

Table A.2 Relation between η and time for various wall thickness $\ell/2$

$$\eta = \frac{1}{\ell}\int_0^{\ell}(1-\theta)\,dx = 1 - \sum_n \frac{8}{(n\pi)^2} e^{-F(n\pi)^2}$$

$$(n=1,\ 3,\ 5,\ 7,\ \cdots)$$

Fourier Number $F = Kt/\ell^2$	Time after Sudden Temperature Rise (S)				η
	$\frac{\ell}{2}$ = 5.5 mm	$\frac{\ell}{2}$ = 40 mm	$\frac{\ell}{2}$ = 130 mm	$\frac{\ell}{2}$ = 210 mm	
0.0001	3×10^{-3}	1.5×10^{-1}	1.6	4.2	0.0220
0.001	3×10^{-2}	1.5	16.2	42	0.0734
0.01	3×10^{-1}	15.3	162	423	0.2257
0.05	1.5	76.5	810	2113	0.504
0.10	2.9	153	1620	4226	0.698
0.20	5.8	307	3239	8452	0.887
0.50	14.5	767	8098	2.11×10^{4}	0.994
1.00	29.0	1533	1.62×10^{4}	4.23×10^{4}	1.000
10.00	289.9	1.53×10^{4}	1.62×10^{5}	4.23×10^{5}	1.000

$K = 4.176 \times 10^{-6}$ (m^2/s) for SUS 304 at 200°C

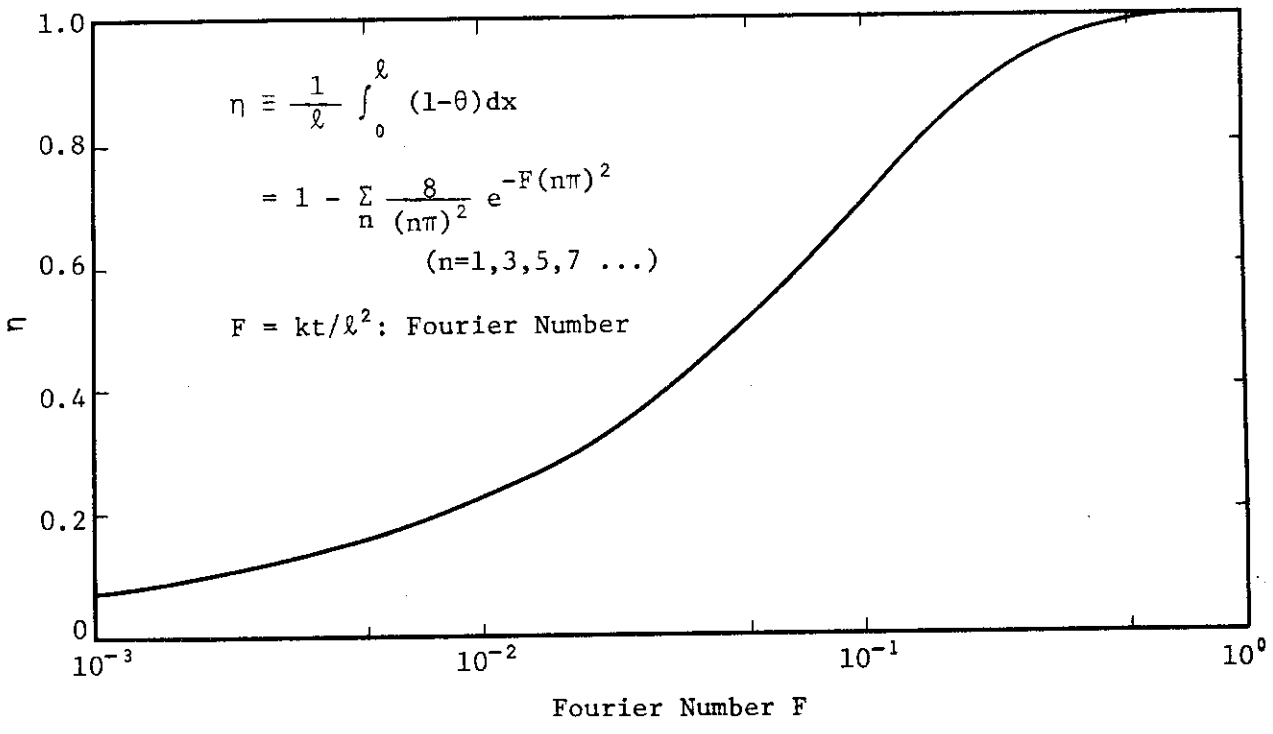

Fig. A.3 η, a degree of approximation to thermal steady state in the case of sudden temperature rise at both surfaces